

Accepted Manuscript

Geological Society, London, Special Publications

Marine bioturbation collapse during Early Jurassic deoxygenation: implications for post-extinction marine ecosystem functioning

Bryony A. Caswell & Liam Herringshaw

DOI: <https://doi.org/10.1144/SP529-2022-226>

To access the most recent version of this article, please click the DOI URL in the line above. When citing this article please include the above DOI.

Received 25 July 2022

Revised 19 December 2022

Accepted 19 December 2022

© 2023 The Author(s). Published by The Geological Society of London. All rights reserved. For permissions: <http://www.geolsoc.org.uk/permissions>. Publishing disclaimer: www.geolsoc.org.uk/pub_ethics

Supplementary material at <https://doi.org/10.6084/m9.figshare.c.6370710>

Manuscript version: Accepted Manuscript

This is a PDF of an unedited manuscript that has been accepted for publication. The manuscript will undergo copyediting, typesetting and correction before it is published in its final form. Please note that during the production process errors may be discovered which could affect the content, and all legal disclaimers that apply to the book series pertain.

Although reasonable efforts have been made to obtain all necessary permissions from third parties to include their copyrighted content within this article, their full citation and copyright line may not be present in this Accepted Manuscript version. Before using any content from this article, please refer to the Version of Record once published for full citation and copyright details, as permissions may be required.

Marine bioturbation collapse during Early Jurassic deoxygenation: implications for post-extinction marine ecosystem functioning

Bryony A. Caswell^{1,2*} and Liam Herringshaw³

¹*School of Environmental Science, University of Hull, Hull HU6 7RX, UK*

²*School of Environmental Science, Griffith University*

³*Hidden Horizons, The Fossil Shop, 65a Eastborough, Scarborough, North Yorkshire, YO11 1NH, UK*

ORCID ID: BAC, 0000-0001-8488-0890; LH, 0000-0001-5216-7126

*Corresponding author (e-mail: b.a.caswell@hull.ac.uk)

Supplementary material: [supplementary figure S1, Table S1 and Table S2] is available at <https://doi.org/10.6084/m9.figshare.c.6370710>

Keywords: Toarcian; Oceanic anoxic event; trace fossil; ichnology, climate change, marine ecosystems

Abstract

Climate change is undermining the health and integrity of seafloor ecosystems, with declines in bioturbation expected to impact future ecosystem functioning. We explored changes in the nature and degree of bioturbation during Early Jurassic global warming and ocean deoxygenation. Understanding how these communities responded can help anticipate how bioturbation and ecosystem functioning might change over large spatial and temporal scales. Trace and body fossils from outcrop and core in the Cleveland Basin, UK show how healthy seafloor communities deteriorated through the Pliensbachian *spinatum* Zone, and macroinfaunal behaviour fluctuated across the Pliensbachian–Toarcian boundary coincident with mass extinction. Deoxygenation began above the stage boundary, and conditions deteriorated until bioturbation ceased completely (upper *tenuicostatum* Zone) for 0.6–2.5 Ma, longer than anywhere else in NW Tethys. The macroinfaunal record revealed new details on the progression and timing of deoxygenation, benthic recovery and fluctuations in the palaeoredox boundary. After the OAE infauna were fewer, smaller and did not mix sediments to depth, whilst the depth and diversity of bioturbation increased by the *fibulatum* Subzone (*bifrons* Zone) the benthos had not recovered to late Pliensbachian pre-OAE state.

Bioturbation collapse over large parts of the northern hemisphere, likely contributed to regional-scale changes in ecosystem functioning.

ACCEPTED MANUSCRIPT

Covering more than 66% of the Earth's surface, seafloor sediments comprise perhaps the largest habitat and species pool on the planet (Snelgrove 1999). They support diverse benthic and pelagic communities, for example by providing habitat and harbouring the benthic resting stages of plankton. These seafloor communities provide a range of important ecological functions, acting as a food source for higher taxa, facilitating the accumulation of sediments, sequestering carbon, and cycling nutrients through marine ecosystems (Snelgrove *et al.* 2014; Solan *et al.* 2019). In turn they support key ecosystem services such as fisheries, waste treatment and assimilation and climate regulation (e.g., Meysman *et al.* 2006; Hattam *et al.* 2015; Aller and Cochran 2019; Solan *et al.* 2020).

Climate change and many other anthropogenic activities are undermining the health and integrity of seafloor ecosystems. One driver of seafloor community change is the loss of oxygen from the oceans, this deoxygenation (ranging from anoxic (no dissolved oxygen) to hypoxic (1–30% dissolved oxygen)) has profound impacts on marine life. For instance, causing mass mortalities of marine animals, declines in organism health, fitness and body-size to name a few (Cheung *et al.* 2013; Riedel *et al.* 2014; Breitburg *et al.* 2018). Dramatic decreases in dissolved oxygen content in the lower water-column and within seafloor sediments result in behavioural changes whereby organisms with low tolerance to deoxygenation vacate the area. As fewer infaunal taxa inhabit the sediment, less sediment mixing occurs, and oxygenation of sediments declines further.

In the last 200 Ma at least nine 'oceanic anoxic events' (OAEs), contemporaneous global periods of deoxygenation represented by enhanced organic carbon-burial and carbon-isotope (c-isotope) excursions have occurred (Jenkyns 2010). These events provide opportunities for exploring how prolonged environmental change, such as deoxygenation, affected seafloor communities and wider marine ecosystems in the past as well as how they may change under future scenarios. We focus here on the early Toarcian oceanic anoxic event (~183 Ma) and preceding changes across the stage boundary in the Cleveland Basin, NE Yorkshire, UK an important reference section for the OAE. This was an Early Jurassic period of (geologically) abrupt and extreme global warming, where seawater temperatures increased by up to 10°C (Bailey *et al.* 2003; Ruebsam *et al.* 2020b) over <500,000 years. Early Toarcian warming was linked to elevated continental weathering (Cohen *et al.* 2004; Them *et al.* 2018), sea-level rise, a large negative C-isotope excursion (up to -6‰ $\delta^{13}\text{C}$) indicating substantial perturbations to the oceanic (Röhl *et al.* 2001; Hermoso *et al.* 2009; Al-Suwaidi *et al.* 2010; Caruthers *et al.* 2011; Gröcke *et al.* 2011; Kemp *et al.* 2011) and atmospheric carbon cycles (Hesselbo *et al.* 2000; Hesselbo *et al.* 2007; Hesselbo and Pienkowski 2011), widespread organic carbon burial (Jenkyns 1988) and global increases in the extent of ocean deoxygenation (Pearce *et al.* 2008; Them *et al.* 2019). These changes were associated with a mass extinction of benthic and

pelagic taxa across the Boreal, Tethyan and Panthalassa oceans (e.g., Little and Benton 1995; Caswell *et al.* 2009; Caruthers *et al.* 2013, Vasseur *et al.* 2021) at the stage boundary and onset of the OAE ((ii) and (iii), Fig. 1). Impoverished low diversity early Toarcian seafloor communities were dominated by tolerant benthic opportunists that underwent large swings in population density and body-size (Caswell and Coe 2013), and macroinfauna were lost in the Cleveland Basin (Caswell and Frid 2017).

The impacts on early Toarcian burrowing marine animals (bioturbators) as represented by the trace fossils that record the *behaviour* of organisms, e.g. movement or feeding, are comparatively less often documented. However, trace fossils can be the only record of taxa with low preservation potential (e.g., those lacking hard parts; e.g. Sperling *et al.* 2013), and past research has highlighted the value of ichnology (the study of trace fossils) in elucidating changes in benthic ecosystems during extinction events (see e.g. Twitchett and Barras 2004; Seilacher *et al.* 2005; Boyer and Droser 2009; Laflamme *et al.* 2013; Hofmann *et al.* 2015; Wiest *et al.* 2015). In this paper, we specifically consider fossil invertebrates (from both body and trace fossils) that inhabited the seafloor and how changes in benthic community composition and behaviour would have contributed to bioturbation during the extreme late Pliensbachian–early Toarcian palaeoenvironmental changes.

Seafloor sediments are mixed to an estimated average depth of 5.75 ± 5.67 cm by burrowing marine animals (Teal *et al.* 2008; Solan *et al.* 2019). This sediment mixing produces a complex and heterogeneous seafloor by aggregating and disaggregating particles and organic matter, changing sediment chemistry, porosity and permeability (e.g., Lohrer *et al.* 2004; Mermillod-Blondin 2011). These processes oxygenate the sediment, enhance the vertical and horizontal transfer of organic matter, establish concentration gradients and increase the sediment surface area available for chemical exchange (Fenchel 1996) which in turn influences the composition of the resident meiofaunal and microbial communities (Warwick and Clarke 1984; Olafsson 2003; Fenchel and Finlay 2008). In well-mixed sediments the degradation of organic matter by deposit feeders, and subsequently aerobic microbes, is enhanced (Kristensen *et al.* 1992; Caliman *et al.* 2007; Bolam and Eggleton 2014; Douglas *et al.* 2017). The richness of the macrofaunal community and the identity, and behaviour, of the species present is strongly correlated with the regeneration of nutrients (Caliman *et al.* 2007; Bulling *et al.* 2010; Snelgrove *et al.* 2018) especially within environments that are not hydrologically dynamic such as the early Jurassic of the Cleveland Basin.

While all burrow-dwelling infauna have the potential to stimulate nutrient cycling, the contributions of taxa vary. Taxa that make the largest contribution to nutrient cycling include those with deep-burrowing and deposit-feeding habits (Snelgrove 1997; Costello *et al.* 2015). It is vital, therefore, to consider trace fossils not just in terms of occurrence and abundance, but also their likely

bioturbation mode(s). Applying the bioturbation classification system of Solan and Wigham (2005) (after Francois *et al.* 1997; Francois *et al.* 2002) to the trace fossil record, Herringshaw *et al.* (2017) argued that taxa that construct galleries at depth in the sediment were the highest-impact burrowing organisms, and emphasized the importance of burrow irrigation to long-term sedimentary oxygenation.

As dissolved oxygen declined during the late Pliensbachian–early Toarcian, so too would the quantity, complexity, and depth of bioturbation. Such patterns have been observed at the present-day: along an oxygenation gradient on the Oman Margin Oxygen Minimum Zone, burrowing is substantially reduced below 0.13–0.27 ml l⁻¹ dissolved oxygen (Demaison and Moore 1980; Smith *et al.* 2000). Changes in burrow size are also useful indicators of environmental stress, and deoxygenation has been linked to reductions in the dimensions of present-day burrows (Smith *et al.* 2000) and trace fossil diameters (their ichnometry; Savrda and Bottjer 1986; McIlroy 2004; Gingras *et al.* 2011).

We quantify the impacts of the late Pliensbachian–early Toarcian palaeoenvironmental changes on macroinfauna, by examining changes in the nature and degree of bioturbation (in outcrop and core) from sediments deposited in the Cleveland Basin, North Yorkshire, UK. Building on the work of Morris (1979), Martin (2004), Caswell and Frid (2017), and Caswell and Dawn (2019), we consider how the nature of bioturbation (i.e. the abundance, diversity, and size of trace fossils) and by inference the diversity and behaviour of the tracemakers themselves, changed during this interval. We compare changes in trace fossils with body fossil diversity and behavioural traits, to better understand the nature and timing of changes on late Pliensbachian–early Toarcian seafloors. These results can yield insights on how seafloor communities and the wider marine ecosystem may change under prolonged deoxygenation in future scenarios.

Materials and methods

Data sources

This study focuses on fossil seafloor communities that are preserved within sedimentary rocks deposited in the Cleveland Basin, a semi-restricted marine basin in NW Europe below storm wave base (>100 m water depth). Trace fossil data were collected from the early Toarcian Whitby Mudstone and late Pliensbachian Cleveland Ironstone formations exposed at geological sections near Saltwick Bay [54°29'15.98"N, 0°35'24.55"W], Port Mulgrave [54°32'51.68"N, 0°46'3.50"W], Staithes [54°33'33.72"N, 0°47'5.29"W], Hawsker Bottoms [54°27'38.75"N, 0°32'46.95"W], Kettleless [54°31'51.66"N, 0°43'2.99"W], Ravenscar [54°24'24.69"N, 0°29'28.12"W] and from core NS1

extracted by Sirius Minerals (now Anglo-American) from the Woodsmith Mine near Doves Nest Farm [54°26'0.22"N, 0°37'18.14"W] approximately 7 km west of Robin Hood's Bay (Supp Fig. S1). The lithology, lithostratigraphy and biostratigraphy for the coastal exposures are from Howarth (1955, 1962, 1973, 1992), Kemp *et al.* (2005, Powell (2010), and for Core N1 is from Trabucho-Alexandre *et al.* (2022) and this study. On the coast the Cleveland Ironstone Formation (Fm.) is composed of pale-grey mudstones with some silty and sandy mudstone units, siderite and berthierine ooidal ironstones. It consists of two units the Penny Nab Member (19 m) and Kettleless Member (10 m) which contain distinctive ironstone seams and nodular siderite horizons (Fig. 1). A very finely laminated mudstone referred to as the "Sulphur Band" (bed 26, Fig. 1; Howarth 1992) occurs where the top of Cleveland Ironstone Fm. meets the overlying c. 100 m thick Whitby Mudstone Fm. The latter is composed of pale- to dark-grey mudstones with occasional bands of laterally persistent calcite or siderite concretions (Fig. 2). The formation is subdivided into the Grey Shale Member (14 m), the Mulgrave Shale Member (29 m) and the Alum Shale Member (37 m, Fig. 2) that differ in colour, siderite nodules, organic carbon and fossil content. The Whitby Mudstone Fm. is unconformably overlain by a condensed ferruginous ooid-rich sandstone the Dogger Fm. (up to 13 m, Fig. 1) on the coast and over much of the basin.

Trace fossil data are a combination of new data collected from coastal exposures in 2010, 2011, 2012, 2013, 2016, 2019 and 2020 (this study) and previous works (Howard 1984; Martin 2004; Caswell 2010; Caswell and Frid 2017; Caswell and Dawn 2019). The data collected span the upper Pliensbachian *Amaltheus margaritatus* and *Pleuroceras spinatum* ammonite zones, and the Toarcian *Dactyloceras tenuicostatum*, *Harpoceras falciferum* and *Dactyloceras bifrons* zones (Fig. 1). Data from the coastal sections comprised information from up to 700 stratigraphic levels throughout 85 m of vertical section (in composite, note the amount of exposure varies between localities and there is overlap between the exposures, Fig. 1), and from 43 stratigraphic levels in 85 m of core N1 examined.

The trace fossil data comprise the number and type of trace fossils observed (the ichnotaxa) at each stratigraphic level, including their size, morphology and orientation, and whether or not they were preserved as pyrite (Table 1). The trace diameters were determined at most levels ($n = 664$) based on measurements of field specimens or from images of field specimens (measured using Image J v. 1.52a, National Institute of Health, USA). Where possible, trace fossils were assigned to ichnogenera and for those that could not be clearly assigned a morphometric scheme was used (Table 1). The trace fossils were interpreted as resulting from locomotion, dwelling or feeding, with the majority suggesting infaunal and not epifaunal activity, no resting traces were observed (Table S1).

Preservation of the trace fossils were recorded as pyritised or not, as when sulfur and iron are abundant body and trace fossils can become partly or completely replaced by pyrite (Scheiber 2002; Gingras *et al.* 2014) where organic material is present (e.g. concentrations of organic matter produced by the animal feeding or defecating within a burrow) and can be indicative of reducing conditions.

The density of trace fossils were classified using the field ichnoindex approach of Droser and Bottjer (1986) where ichnofabric: 1 = zero evidence for bioturbation; 2 = <10% bioturbated; 3 = 10-40% bioturbated; 4 = 40-60% bioturbated; 5 = >60% bioturbated. In homogenized mudstones where discrete traces were not observed an ichnofabric score of 2 was used, and the presence of laminae was also recorded (as 1= laminae present, 2 = laminae absent) to account for cryptobioturbation (subtle very small-scale disruption of grain fabrics by amphipods; e.g., Pemberton *et al.* 2008). The indices were assigned based on macroscopic trace fossils that could be discriminated in the field or in core on the basis of lithological or mineralogical changes (the presence of meiofauna is not excluded although no pyritised meiofaunal traces were observed). If the primary data did not report an ichnofabric index then data were converted to this scheme as far as was possible, e.g. from % rock borrowed (Caswell and Frid 2017; Caswell and Dawn 2019) or relative abundance scores (Howard 1984). For instance, facies where ichnotaxa occurred or were rare (in the relative abundance scheme of Howard 1984) an ichnofabric score of 2 was assigned for that ichnotaxon, when trace fossils were 'common' a score of 3 was assigned, very common trace fossils were assigned a score of 4 and abundant trace fossils were assigned a score of 5. The ichnofabric score for the facies was determined from the median score across all of the ichnogenera present

The trace fossil data are presented separately for outcrop and core, and comparisons between the two are made with some caution. It is likely that fine details (i.e. laminations and faint ichnotaxa) will be more visible in the cut surface of the core, and so smaller trace fossils may be more noticeable in core whilst larger trace fossils may not be captured in such a spatially constrained area (5 cm diameter). By contrast the collection of data at outcrop although more time consuming, has a number of advantages because it spans a much greater spatial area, and although larger trace fossils will be obvious the fine details may not. Using a combination of data from outcrop and core can give a more complete picture than using just one or the other, and it provides a wider spatial picture of changes on the seafloor.

Interpretations from trace fossils differ from body fossils because they record behaviours rather than species identities, and several species may produce what appears to be the same trace and so some uncertainty will always exist surrounding trace-maker identity (Seilacher 2007; Bertling 2011). Consideration of the biological traits used in this study is advantageous because it focusses on measurable attributes or behaviours (Supplementary Material Table S1) which can be compared with the behaviour of present-day taxa, and does not depend overly on species identities. The behaviour expressed by a tracemaker can vary with sediment type and so caution should be used, although this probably was not the case in the present study, because lithology varied little through time (Fig. 2).

Biological traits classification

The attributes of the trace fossils were described using Biological Traits Analysis (Bremner *et al.* 2006). Biological traits were selected that described measured and observable features of aspects of trace fossil morphology (modified from Caswell and Frid 2017), including: the maximum trace diameter, gross morphology, orientation, maximum depth of the vertical components (Traits A–D, Table 2). A further four features were used to capture detailed information on the tracemakers (Traits E–H, Table 1), these were: the presence and nature of a burrow lining (if present); evidence for excavation (spreiten, faecal pellets, menisci); the presence or absence of burrow ornamentation known as bioglyphs (Ekdale and De Gibert 2010); and, the burrow complexity, where those that were multi-dimensional, multi-branched, and with multiple openings were considered more complex. Each trait was divided into 3–6 categories, referred to as ‘modalities’. For example, trace *gross morphology* was subdivided into: (H1) unbranched, (H2) intermittent branching, (H3) regular branching and (H4) highly branched based on the number branches per section of trace (Table 2).

After each ichnotaxon was classified morphologically (Traits A–H, Table 1), the palaeoecology of the tracemakers were interpreted. Published accounts of the trace fossil ethology and information on the behaviour of present-day marine benthos guided the selection of traits used and the rationale for interpretations of behaviour (Gingras *et al.* 2008; Dashtgard and Gingras 2012; MacEahern *et al.* 2012). The rationale for species assignments is available in Table 2 (see also supplementary Table S1 for details on each ichnotaxon and morphotype).

The behavioural traits included feeding mode, minimum likely sediment depth, likelihood of burrow irrigation by the animal, and the bioturbatory modes (Traits I–L, Table 2). Feeding mode was classified as: (I1) deposit feeders or grazers, i.e. those that consume particulate organic matter, bacteria or benthic algae from sediments; (I2) suspension/filter feeders that extract nutrition from the water column; and, (I3) predator/scavengers that consume living or dead animal tissue. The

minimum likely sediment depth inhabited was assigned using categories modified from Bambach *et al.* (2007) as (J1) surface traces; (J2) semi-infaunal (0–5.0 mm) whereby the tracemaker was partly infaunal and partly exposed to the water column; (J3) shallow infaunal (5.01–50 mm); and, (J4) deep infaunal (>50.01 mm). The likelihood that a trace was bioirrigated was considered to be: (K1) highly improbable (surficial locomotion or grazing traces with full access to the oxygenated water-column); (K2) improbable (semi-infaunal forms for which irrigation is unlikely to be needed); (K3) probable, for shallow, simple burrows, possible dwelling structures, which might have required at least short-term irrigation; or (K4) required for ichnotaxa with deeper and/or more complex burrow systems in which irrigation is likely to have been required for long term occupation. As well as burrow depth and complexity, the presence of a burrow lining can reflect a difference between an oxygenated interior and exterior.

Finally, the likely bioturbatory functional group(s) to which the tracemaker belonged was assigned. Using this functional group classification, interpretations can be made about the inferred relative contribution to sedimentary particle and nutrient fluxes associated with each. The six trait modalities used to capture bioturbatory modes were modified from Solan *et al.* (2004); Solan and Wigham (2005); Herringshaw *et al.* (2017), and were as follows:

- (1) **Epifaunal locomotion:** minor disturbance at or above the sediment-water interface (but not penetration of the sediment) primarily by an organism moving. This can include trackways and resting traces, none of which were observed in the present-study.
- (2) **Surficial modification:** slightly greater disturbance than (1) which includes both locomotion and feeding. Includes organism(s) producing discrete horizontal surface traces as they move shallowly across the sediment, e.g. surface grazing trails.
- (3) **Biodiffusive mixing:** where sediment is thoroughly bioturbated without structure. Interpreted as homogenised deposits, e.g. without lamination, and discrete burrows are absent ($ii \leq 1$).
- (4) **Upward conveying/regeneration:** The former describes an organism feeding in the sediment, and moving material to the surface, this behaviour can be identified by oblique-to-vertical burrows within which the organism feeds. The latter describes the excavation and relocation of sediments to the surface, after which vacant burrows become passively filled. Both behaviours are likely to result from deposit feeding and/or substantial excavation to create a subsurface structure. The presence

of spreiten (produced by within-burrow movement), menisci (backfill) and bioglyphs (e.g. scratches, (Ekdale and De Gibert 2010)) in burrows reflects excavation or the reworking of sediment for food (e.g., Seilacher 2007; Dashtgard and Gingras 2012). Both behaviours produce oblique-to-vertical burrows. It is not possible to distinguish these two behaviours from each other in the fossil record, as any casts or pseudofaeces deposited on the sediment surface are unlikely to be preserved (Savrda 2007).

- (5) **Downward conveying:** the opposite of upward conveying, this behaviour can be identified by oblique-to-vertical burrows within which the organism excretes waste products, i.e. with faecal pellets present in the burrow.
- (6) **Gallery biodiffusion/bioirrigation:** Complex burrows that are mid-deep in the sediment with both vertical and horizontal components, the burrows are expected to require irrigation and there will likely be evidence of excavation and perhaps feeding.

Each ichnotaxon was scored for its affinity to each modality ranging from 0–1 (0= no affinity to 1 = high affinity) using the ‘fuzzy scoring’ method (Chevene *et al.* 1994) to capture multiple trait modalities. For instance, for taxa exhibiting multiple behaviours or where behaviour is uncertain. The traits of each ichnotaxon or morphotype were determined from observation and measurement of specimens. These were verified for each ichnogenera using descriptions of morphology and interpretations of their palaeobiology within the published literature (for sources of information and taxon classification see Supplementary Material Table S1). Within any one stratigraphic level, the abundance of each behavioural trait modality (Traits I–L, Table 2) was calculated by weighting the modality scores (supplementary Table S2) by the abundance of each ichnotaxon exhibiting that modality. This produced an abundance weighted score for each modality from each point in time. The number of bioturbatory modes were also determined for each level.

The trace fossil assemblage was compared with relative changes in body fossil diversity and abundance, additionally the abundance of the different feeding modes and minimum likely sediment dwelling depths of body and trace fossils were also compared to achieve an integrated picture of changes in seafloor assemblages. Body fossil abundances (fossil counts) and diversity from the Cleveland Ironstone and Whitby Mudstone formations (from 415 stratigraphic sample points) at outcrop on the NE Yorkshire coast (supplementary Fig. S1), are combined from Little (1996); Caswell

et al. (2009); Caswell (2010); Caswell and Coe 2013; Danise *et al.* (2013); Caswell and Dawn (2019). Data on the distribution of trait modalities are from Caswell and Frid (2017). Geochemical context is provided by data collected from the same coastal outcrops and are compiled from Saalen *et al.* (1996), Harding (2004), Kemp *et al.* (2005), Pearce *et al.* (2008) Littler *et al.* (2010) Kemp *et al.* (2011), Korte and Hesselbo (2011) (Fig. 1).

The trace fossil assemblages from the different temporal points were compared using the ichnodiversity, ichnofabric index, trace fossil diameter and number of bioturbatory modes represented. Kruskal Wallis tests were used to compare the median values for each ammonite subzone. The relationships between the different metrics were compared using linear regression. Statistical analyses were carried out in SPSS v. 22 (IBM Corp).

Results

The coastal outcrops

Upper Pliensbachian–lower Toarcian. Within the upper part of the *Pliensbachian* (Cleveland Ironstone Fm.) exposed on the coast, 12 ichnotaxa occurred (Fig. 2) including *Chondrites*, *Diplocraterion*, *Ophiomorpha*, ?*Ophiomorpha*, *Palaeophycus*, *Phoebichnus*, *Planolites*, *Phycosiphon*, *Rhizocorallium*, *Teichichnus*, *Thalassinoides* (Figs 3–4); and Howard (1984) reported often pyritised “pellet stuffed” burrows (referred to as “Type A”) from Hawsker Bottoms. Aside from Type A and *Phoebichnus*, all of these ichnotaxa were observed at Hawsker Bottoms, Staithes and Kettleiness (Fig. 2). In places *Ophiomorpha* occurred as single unbranched shafts (Fig. 4J), individual excavations such as these are uncommon and may indicate initial stages of construction (Frey *et al.* 1978). In addition, largely structureless annulated pyritised masses were recorded from Kettleiness (Fig. 4K), and whilst these seemed to have an affinity with *Ophiomorpha* (Fig. 4I) and occurred within similar horizons they did not fit the linear annulated form described for the ichnogenera (Frey *et al.* 1978) and so were recorded separately as ?*Ophiomorpha*. They had some similarity to the small annulated mounds found at the burrow openings of *Callianassa major* on beaches in Georgia, this species is one of the proposed present-day tracemakers for *the ichnogenera* (Frey *et al.* 1978).

A maximum of 6 ichnotaxa, including both vertical and horizontal morphologies, occur within any one stratigraphic level of the upper Pliensbachian (Fig. 5). The median number of ichnotaxa recorded per stratigraphic level significantly differed throughout the section studied (Kruskal-Wallis test $Z = 460.16$, $df = 11$, $p < 0.001$). Two to three ichnotaxa occurred in the *Amaltheus gibbosus* Subzone, and ichnodiversity doubled in the *apyrenum* Subzone with four or more ichnotaxa in most horizons. In the lower *Pleuroceras hawskerense* Subzone two ichnotaxa occur in most horizons, and just below

the Pliensbachian–Toarcian boundary the number of ichnotaxa became highly variable, fluctuating between 0 and 6 ichnotaxa at any one level (Fig. 5, Table 3). Pairwise Kruskal-Wallis comparisons showed that the median number of ichnotaxa observed in the Pliensbachian (*gibbosus*–*hawskerense* subzones) did not differ from each other nor the lowermost Toarcian subzone, but did contain significantly more ichnotaxa than present in any horizon of the following six ammonite subzones (*Protogrammoceras paltum*–*Dactyloceras commune*, Table 3).

The changes in ichnodiversity coincided with fluctuations in the intensity of bioturbation as indicated by the ichnofabric index. The median ichnofabric index per stratigraphic level significantly differed between ammonite subzones (Kruskal-Wallis test $Z = 465.10$, $df = 11$, $p < 0.001$). Facies of the *gibbosus* Subzone were <10% bioturbated ($ii = 1$ – 2 , Fig. 5) whereas most of the *apyrenum* and *hawskerense* subzones were between 10–40% and >60% bioturbated ($ii = 3$ – 5 , Fig. 4G–I, Fig. 5), although the median ichnofabric index did not significantly differ between the three subzones (Kruskal-Wallis Pairwise, $p > 0.05$). Similar to ichnotaxa number, the amount of bioturbation became much more variable just below the Pliensbachian–Toarcian boundary (from bed 39), ranging between 0% and >60% bioturbated (Fig. 5). Most facies of the upper Pliensbachian were homogenised, but in some beds (40–42, 26, 1–2; Fig. 5) finely laminated intervals occurred. At the stage boundary, the well-bioturbated grey shales ($ii = 5$) of bed 25 became more frequently laminated (Fig. 4F), and were very finely laminated ($ii = 1$, Fig. 4E, 5) at the stage boundary in bed 26 (the “Sulphur Band”). Towards the top of bed 26, *Rhizocorallium* appears ($ii = 2$; Fig. 3E) and near the bed 26–27 boundary *Diplocraterion* was observed (Fig. 3C–D). The bed 27 specimens have an initially vertical U-shaped *Diplocraterion*-like morphology, but deviate into an obliquely oriented *Rhizocorallium* morphology (Fig. 3C–D; Herringshaw *et al.* In review) typically referred to as *Rhizocorallium jenense* (Fürsich 1974). The shift to oblique forms could reflect a shift from predominantly deposit feeding (horizontal forms) to mixed deposit and suspension feeding (oblique forms) (Schlirf 2011) related to palaeoenvironmental change.

The maximum diameter of trace fossils ranged from millimetric *Planolites* and *Chondrites* up to 60 mm *Thalassinoides* just below the Pliensbachian/Toarcian boundary. Trace fossils declined to <10 mm diameter above bed 3 in the *paltum* Subzone. Median trace fossil diameter significantly varied between ammonite subzones (Kruskal-Wallis test $Z = 420.60$, $df = 11$, $p < 0.001$), pairwise tests showed that although Pliensbachian traces did not significantly differ in size from each other, traces in the *hawskerense* and *gibbosus* subzones were of similar size to those present in lowermost Toarcian (Table 3), whereas trace fossils in the *apyrenum* Subzone were typically larger.

The number of bioturbatory modes represented in the upper Pliensbachian trace fossil assemblages was significantly higher than in the lower Toarcian (from the *Dactyloceras clevelandicum* Subzone onwards; Table 4, Fig. 6). The trace fossils present in the *gibbosus* Subzone were mostly those of tracemakers that were active on the sediment surface, in the *apyrenum* Subzone shallow burrowers (5–50 mm) predominated, and in the lower half of the *Pleuroceras hawskerense* Subzone traces representing both deep (>50 mm) and shallow burrowers occurred. In the middle *hawskerense* this switched to predominantly shallow burrowers, followed by mostly deep burrowers in the upper *hawskerense*. All bioturbatory modes were represented in the upper Pliensbachian trace fossil assemblage, except for epifaunal locomotion (as no resting traces or trackways were observed), snail grazing trails (classified as surface modifiers, L2) occasionally occurred (Fig. 6). Trace fossils from the *gibbosus* Subzone indicated that a small amount of surface disturbance and downward conveyance of sediment was occurring, whereas in the *Pleuroceras apyrenum* Subzone most trace fossils were those of ichnotaxa thought to mix sediments by biodiffusion. This is consistent with the predominantly homogenised sediments observed within this interval (Fig. 5). The greatest number of bioturbatory modes occurred in the upper *apyrenum* and *hawskerense* subzones (Table 3, Fig. 6), with downward conveyors, upward conveyors/regenerators and gallery biodiffusors becoming more prominent and biodiffusors less so.

In the lower Toarcian *tenuicostatum* Zone *Chondrites* is preserved in mudrock and occasionally siderite nodules, with *Planolites* occurring in the lower part. Near the top of the *tenuicostatum* Zone occasional *Rhizocorallium* (Fig. 4H) and *Planolites* occurred and pyritised ?*Ophiomorpha* were common in beds 25–29 (Fig. 2, Fig. 4I–J). We did not observe branched forms, so we tentatively assign these to the genus *Ophiomorpha*. As for the *spinatum* Zone, much of the lower part of the *tenuicostatum* Zone was homogenised, but in some beds (26, 2 and 19 of the *paltum* and *clevelandicum* subzones) the facies were laminated showing that disturbance was minimal (Fig. 2).

Ichnodiversity declines throughout the *tenuicostatum* Zone, the *paltum*–*Dactyloceras semicelatum* subzones (Fig. 2, Table 3) had significantly lower median number of ichnotaxa than were present in the late Pliensbachian facies (Kruskal-Wallis pairwise test $p > 0.05$, Fig. 2, Table 3). Similar to ichnodiversity, the amount of bioturbation declined to <40% bioturbated and some horizons were completely unbioturbated (Fig. 2). The median ichnofabric index in the earliest Toarcian (*paltum*–*semicelatum* subzones) was 2–3 times lower (Kruskal-Wallis pairwise test $p > 0.05$) than in the late Pliensbachian (*apyrenum*–*hawskerense* subzones, Fig. 5, Table 3). Trace fossil diameters were initially small, with slightly larger, up to 40 mm, ?*Ophiomorpha* and *Rhizocorallium* in the *tenuicostatum*–*semicelatum* subzones. Where trace fossils occurred, both vertical and horizontal

traces tend to be present, but in some stratigraphic levels only horizontally oriented forms were observed (Fig. 5).

Trace fossils representing deep infauna were abundant in the *paltum* Subzone with a small amount of shallow infauna (Fig. 5). In the *clevelandicum* and *tenuicostatum* subzones few trace fossils were observed, but those that occurred were a mixture of deep and shallow burrowing forms. *Paltum* Subzone sediments varied between being laminated and being homogenised, with most bioturbators mixing sediments by upward conveyance/regeneration, downward conveyance and gallery networks, with biodiffusion being less common (Fig. 5). In the *clevelandicum*–*semicelatum* subzones where trace fossils occurred, bioturbation would have consisted of a small amount of downward conveyance, upward conveyance/regeneration and gallery biodiffusion.

The taxonomic diversity of benthic body fossils broadly covaried with trace fossil diversity (Fig. 5), even though the two records differ in that the latter represents the number of distinct behaviours present rather than the number of species. The diversity of both body and trace fossils was higher in the late Pliensbachian and declined in the early Toarcian (*paltum*–*tenuicostatum* subzones), followed by a diversity peak in (with 15 bivalve species and one ichnotaxa) the *semicelatum* Subzone prior to the start of the OAE (Fig. 5).

The Toarcian Oceanic Anoxic Event. Above the bed 31 lithology change in the *semicelatum* Subzone the facies become laminated and, in all but a few discrete thin horizons in beds 47 and 49, remain this way throughout most of the *falciferum* Zone and the lower half of the *commune* Subzone. The ichnofabric index also indicates an almost complete absence of bioturbation. Trace fossils are very rare throughout the 42 m of vertical section, body fossils of epifaunal bivalves are often very abundant (Fig. 5). *Bositra radiata* appears once trace fossils disappear and dominates until extinction horizon (iii) when it switches to *Pseudomytiloides dubius* (Caswell and Coe 2013).

During the *Cleviceras exaratum*–*Harpoceras falciferum* subzones the median number of ichnotaxa at any one stratigraphic level did not significantly differ from those present in the *clevelandicum* and *tenuicostatum* subzones (where trace fossils are also very rare), but was significantly lower than in any other subzones (pairwise K-W, $p > 0.05$, Table 3). The ichnofabric index was also significantly lower than in any other subzone, except for the *clevelandicum* Subzone (Table 3). In bed 38 near the end of the OAE, the infaunal bivalve *Goniomya rhombifera* makes a brief appearance (Fig. 6, Caswell *et al.* 2009).

From the middle *falciferum* Subzone up until the middle *commune* Subzone body fossils become far less abundant, with individual bivalves occurring occasionally (Fig. 5). Small pyritised branching burrows occur (*Trichichnus* sp. A; Fig. 2, Fig. 4G) within the top of the Ovatum Band (bed 48) at Saltwick Bay only and so any burrowing was spatially limited. At approximately the same level the semi-infaunal brachiopod *Lingularia longovicensis* occurs (Caswell *et al.* 2009).

Recovery from the Toarcian Oceanic Anoxic Event. In total 15 ichnotaxa were observed throughout the *bifrons* Zone, four could be associated with established ichnogenera (*Rhizocorallium*, *Palaeophycus*, *Chondrites*, ?*Trichichnus* sp. A, ?*Trichichnus* sp. B, ?*Trichichnus* sp. C, *Thalassinoides* and ?*Ophiomorpha*; Fig. 4A–F) and a further 7 that did not occur lower in the coastal outcrops (Fig. 2) were classified as morphotypes (Table 1–2, Table S2).

Three trace fossil types that share similarities with *Trichichnus* were found in the *bifrons* Zone at Saltwick Bay and Ravenscar (Fig. 2). They are distinguished based on trace diameter, sp. A was <3 mm diameter, sp. B 5–10 mm, and sp. C >10 mm. *Trichichnus* is a fine (0.1–0.7 mm diameter), branched or unbranched, winding trace fossil reported from fine grained sedimentary rocks where it is often preserved as pyrite (Frey 1970; Kedzierski *et al.* 2015). Assignment of the Toarcian specimens to *Trichichnus* is uncertain because they are of much larger diameter and all were parallel with the bedding whereas *Trichichnus* is usually vertically oriented.

Recolonisation of the benthos began with body fossils starting to become more numerous in the middle of bed 51, and were mostly comprised the infaunal deposit feeding bivalve *Dacryomya ovum*. Midway through the *commune* Subzone, trace fossils reappeared (base of bed 53) and at any one stratigraphic level up to three ichnotaxa were observed. Ichnodiversity in the *commune* Subzone did not significantly differ from the *paltum–tenuicostatum* subzones, it was significantly higher than during the OAE but was lower than in the late Pliensbachian (Fig. 2, Table 3).

Many stratigraphic levels of the *bifrons* Zone only contained horizontally oriented burrows, with vertically oriented trace fossils being far less common than before the OAE. For instance, 20–34% of the stratigraphic levels examined in the *Peronoceras fibulatum* and *Catacoeloceras crassum* subzones contained vertically oriented trace fossils compared with 76–100% of those from lower in the section (*gibbosus–clevelandicum* subzones; Fig. 5). Furthermore, much of the upper *bifrons* Zone was homogenised, with laminated facies occurring intermittently in two main intervals (in beds 55–63 and 72; Fig. 5) which corresponded with a generally lower ichnofabric index. At many discrete

intervals within the bioturbated part of the *bifrons* Zone trace fossils were predominantly pyritised (Fig. 5).

The ichnofabric index was initially high (10–60% bioturbated) in the mid-*commune* Subzone, then decreased to <10% bioturbated from the middle of bed 53 up to bed 55, the median ichnofabric index was 0.5 (where 1 ≤10% bioturbated) and was comparable to the *gibbosus* and *clevelandicum–tenuicostatum* subzones. Both the number of ichnotaxa and the ichnofabric index were very variable (Fig. 5). In the *bifrons* Zone the first trace fossils to appear (in the lower part of bed 53) were up to 20 mm in diameter, they then remained small (<10 mm) throughout the remainder of bed 53 until bed 63 when they double in size.

The trace fossils of the *commune* Subzone reflected tracemaker activity at the sediment surface only, this was followed by intermittently occurring shallow burrowing forms.

Epifaunal trace fossils were rare throughout the whole succession, they were limited to grazing trails in the *bifrons* Zone, and it is unlikely that the surface layer was completely preserved because in these settings where sedimentation rates are low they are usually removed, e.g. by currents, or “overprinting” by bioturbation prior to burial (Savrda 2007). Although preservation of the mixed layer is more likely in anoxic areas where bioturbation ceases for extended periods, it is likely that tracemaker surface activity is under-represented (e.g. tracks, trails, surface deposited pellets or chimneys).

In the *fibulatum* Subzone more ichnotaxa began to occur and bioturbation was often higher (ii >10–40%) and less variable than in the *commune* Subzone. Although 2–4 times more taxa were found in the late Pliensbachian, the median ichnodiversity in the *fibulatum–crassum* subzones did not significantly differ from that at most horizons in the *gibbosus–hawskerense* subzone (Table 3, Fig. 5). In the upper part of bed 72 (*crassum* Subzone) large sand and pebble filled *Thalassinoides* of up to 80 mm diameter can be observed within the base of the Dogger Fm. (Fig. 2, Fig. 4A–B) between Saltwick Bay and Whitby. These *Thalassinoides* (also observed by Powell (2010)) cut down a metre or so into the upper part of bed 72 and seem to originate from the Aalenian Dogger Fm. (Fig. 4A–B). The *Thalassinoides* could therefore have formed at any point during the ~4 Ma unconformity and given that the lithologies are very different from the Whitby Mudstone Fm. in the Cleveland Basin, and other areas at this time (Howarth 1992), they are excluded from any interpretations of palaeoenvironmental change in the early Toarcian.

Trace fossil diameter fluctuated throughout the *fibulatum* and *crassum* subzones (Fig. 5), they did not differ in size from those in the *paltum–tenuicostatum*, but they were significantly smaller than those in the *apyrenum–hawskerense* subzones (Table 3). The amount of bioturbation, as indicated by the ichnofabric index, in the *fibulatum–crassum* subzones was also comparable to that in the upper Pliensbachian and lower Toarcian *gibbosus*, *hawskerense* and *paltum* subzones (Table 3, Fig. 5). Although fewer bioturbatory modes were represented in the *fibulatum–crassum* subzone trace fossil assemblage, the median number did not statistically differ from the upper Pliensbachian (Table 3, Fig. 6). The majority of trace fossils in the *fibulatum* Subzone were those produced by tracemakers living on the sediment surface or at shallow depths, with most bioturbation being surface modification, some biodiffusive mixing and a small amount of upward/downward conveyance (Fig. 6). Whereas in the *crassum* Subzone, surface and shallow infauna occurred in similar abundances, with a smaller amount of deep burrowing. A greater degree of vertical mixing occurred in the *crassum* Subzone with all bioturbatory modes being observed, except for epifaunal locomotion (Fig. 6). After the OAE body fossils were mostly those of deposit feeders/grazers (*D. ovum*) and tracemakers were interpreted to be a mixture of deposit feeders/grazers and suspension/filter feeders, this is in contrast with the upper Pliensbachian and lower Toarcian where most tracemakers were deposit feeders/grazers (Fig. 6).

Although both were more variable, the ichnodiversity and the ichnofabric index of the *crassum* Subzone trace fossil assemblages were comparable with that present before the OAE (Fig. 5). They were significantly smaller than tracemakers in the *apyrenum–hawskerense* subzones. The bioturbatory modes of the tracemakers were similar although there was more surface modification and less deep burrowing, biodiffusive mixing and gallery construction in the *fibulatum–crassum* subzones than in the upper Pliensbachian (*spinatum* Zone). The *fibulatum–crassum* subzones trace fossil assemblages also had more equal proportions of suspension and deposit feeders (Fig. 6).

The N1 Core

A total of ten ichnotaxa were found in core N1. In the upper Pliensbachian *Rhizocorallium*, *Chondrites*, *Planolites*, *Diplocraterion*, *Teichichnus* and the 3–5 mm, 5–10 mm and >10 mm diameter horizontally oriented morphotypes were found in the *apyrenum* to lower *paltum* subzones (Table 1, Fig. 2). In the *paltum–tenuicostatum* subzones only the <3 mm morphotype occurred. No traces fossils were found in the *semicelatum–falciferum* subzones. In the upper part of the core (*commune–fibulatum* subzones) *Chondrites*, the <3 mm, 3–5 mm, 5–10 mm and >10 mm diameter horizontally oriented morphotypes were found together with a <3 mm horizontally oriented annulated form (Fig. 2).

Although the trace fossil data from core N1 are fewer ($n = 43$) and of narrower stratigraphic range (i.e., from the upper *apyrenum* to the *fibulatum* subzones) than those from the coastal exposures ($n = 700$, from the *gibbosus*–*crassum* subzones), the six NE Yorkshire coastal sections and core N1 showed similar changes through time (Fig. 5), notably that:

- At most levels the *spinatum* Zone is well bioturbated ($ii = 2$ – 5) with 1–4 ichnotaxa present including both horizontally and vertically oriented forms. Ichnotaxa number and ichnofabric index fluctuate more near the stage boundary. Trace fossil diameter is on the order of 20 mm and gradually decreases until trace fossils disappear in the *tenuicostatum* Subzone (Fig. 5).
- The *tenuicostatum* Subzone contains fewer ichnotaxa (one or less), and is <10% bioturbated ($ii = 2$, Fig. 5). Only horizontally oriented trace fossils are observed and it is laminated throughout.
- The entire *falciferum* Zone up to the lower third of the *bifrons* Zone contains no evidence for bioturbation ($ii=1$, ichnotaxa = 0), this interval is approximately 42 m thick on the coast and 45 m thick in the core and is laminated throughout (Fig. 5).
- In the upper part of the *commune* Subzone one ichnotaxa appears and facies have an ii of 2. As was observed at the coastal sections, both the number of ichnotaxa and ii increase in the *fibulatum* Subzone which contains 1–2 ichnotaxa, at any one stratigraphic level, and ii is <10% at some horizons with >60% in others. Trace fossils attain a maximum of 10 mm diameter only, with the largest occurring in the upper Alum Shales. As observed from the coastal sections, the majority of trace fossils are horizontally oriented with some vertically oriented morphologies being observed towards the top of the core.
- In terms of tracemaker behaviour, before the OAE most tracemakers were deposit feeders/grazers both on the coast and in the core, and afterwards a mixture of deposit feeders/grazers and suspension/filter feeders occurred (Fig. 6). It is also apparent that below the stage boundary both records showed a transition from shallow to deeper burrowing ichnotaxa (Fig. 6). Similarly, in the upper Pliensbachian bioturbation developed from biodiffusive mixing only to include vertical conveyance (up and down) of sediments and gallery biodiffusion. The number of bioturbatory modes declined to zero during the lower Toarcian, as ichnotaxa disappeared (mid-

semicelatum Subzone; Table 3, Fig. 6). In the *commune* Subzone after the OAE semi-infaunal tracemakers that modified surface sediments predominated with some gallery biodiffusion and upward conveyance/regeneration of sediments.

The overall record from the N1 core differs somewhat from the coastal exposures in having: (1) a maximum of 4 ichnotaxa within any one stratigraphic level, whereas a total of 6 were observed at the coast; (2) trace fossils were generally smaller, 20 mm diameter maximum compared with 60 mm on the coast; (3) pyritised trace fossil were not found in the Pliensbachian facies from the core, unlike in the coastal sections; (4) the *tenuicostatum* Zone was laminated throughout the core, with just the upper part appearing laminated in the coastal outcrops. Furthermore, traits data show that changes in tracemaker behaviour also varied slightly between the records from the core and the coastal sections. In the core a transition from shallow-deep infauna to semi-infaunal ichnotaxa which bioturbate by surface modification occurs before the OAE (in the *paltum* Subzone) that is not apparent on the coast (Fig. 6). Conversely, on the coast ichnotaxa with shallow burrowing habits are more prevalent both before and after the OAE, occurring in similar or greater proportions than surface modifiers.

Relationships between ichnodiversity, tracemaker body-size, amount and nature of bioturbation

Ichnodiversity and ichnofabric index at outcrop (Fig. 5) were positively correlated with each other ($R^2 = 0.555$, $F = 838$, $p < 0.001$), a greater number of trace fossil morphologies occurred within stratigraphic levels that were more obviously bioturbated. Trace fossil diameter, within any one time-averaged stratigraphic horizon, was positively correlated with the ichnotaxa number ($R^2 = 0.305$, $F = 296$, $p < 0.001$) and the ichnofabric index ($R^2 = 0.329$, $F = 319$, $p < 0.001$). This reflects the co-occurrence of a greater number of burrow morphologies, of larger size, at times when there was a greater degree of bioturbation. The number of burrow morphologies (linear regression, $R^2 = 0.371$, $F = 406.41$, $p < 0.001$) and ichnofabric index ($R^2 = 0.4441$, $F = 530.80$, $p < 0.001$) were also correlated with the number of bioturbatory modes present. In the *apyrenum*, *hawskerense* and *crassum* subzones when ichnodiversity and the ichnofabric index were highest 3–5 out of the six possible bioturbatory modes were possible.

Ichnodiversity in the core was also positively correlated with the ichnofabric index ($R^2 = 0.760$, $F = 126.80$, $p < 0.001$) and maximum trace fossil diameter ($R^2 = 0.60$, $F = 59.81$, $p < 0.001$). Maximum trace fossil diameter was also correlated with the ichnofabric index

($R^2 = 0.60$, $F=60.05$, $p<0.001$). The number of possible bioturbatory modes present in the assemblage did not correlate with the ichnodiversity, ichnofabric index, nor the maximum trace diameter, perhaps due to the smaller number of trace fossils observed in the core (attributable to preservational/observational bias when examining core material).

Discussion

As the Earth has warmed, ocean oxygen content has decreased $>0.43\%$ every year for the last 50 years (Stramma *et al.* 2010), this has been exacerbated by over-fertilisation of the oceans from human activities (Diaz and Rosenberg 2008). Models predict that under high CO_2 emissions scenarios there will be an ongoing decline in dissolved oxygen of $>7\%$ from the present-day until 2100 (Keeling *et al.* 2010). These emissions scenarios also predict a 7.5°C atmospheric temperature rise by 2100 (IPCC 2013) making these changes comparable with early Toarcian warming. Thus, changes across the late Pliensbachian–early Toarcian can be a valuable analogue for future predictions of ecosystem change. Examination of the trace fossil record from the NE Yorkshire in the present study provides a detailed picture of how the Cleveland Basin seafloor responded to early Jurassic warming and deoxygenation.

We follow, the decline and complete disappearance of a diverse infauna during the late Pliensbachian and the early Toarcian oceanic anoxic event using high–resolution macroscopic trace and body fossil records. With the exception of one very limited occurrence at the *falciferum–bifrons* Zone boundary, the seafloor remained species poor and without infauna for 1–2 million years. Shifts towards communities dominated by surface dwelling suspension feeders, although not typical in deoxygenated areas today, are similar to those inhabiting deoxygenated parts of the present day seafloor in Kiel Bay, the Bornholm Basin (Karlson *et al.* 2002), and Chesapeake Bay (Dauer *et al.* 1992) where bivalves with adaptations (e.g., *Arctica islandica*, *Astarte borealis*, *Macoma* spp., *Varicorbula gibba* and *Mulinia lateralis*) for surviving hypoxia dominate. Once tracemakers re-emerged after the OAE burrowing was less intense, the macroinfaunal assemblage was very different, their burrows were half the size and less complex, penetrating sediments to < 50 mm, with a narrower range of bioturbatory modes than those present in the late Pliensbachian. The large shifts in the composition and behaviour of benthic communities during the OAE would have had large scale consequences for Toarcian ecosystem functioning, including biogeochemical cycling, primary and secondary production, biogenic habitat provision and food web dynamics.

Changes through time

Changes in Early Jurassic systems during the OAE were complex, and many questions remain about the onset and recovery from the event (Caswell and Frid 2017; Reolid *et al.* 2021a), drivers and variations in space, both locally and globally (Ruebsam *et al.* 2020a). The impacts on early Toarcian bioturbators are not yet as well-studied as the geochemical or palaeontological trends from body fossils. Recently, Rodríguez-Tovar (2021) reviewed trace fossil records across the Toarcian OAE and demonstrated that the quality of the record differs greatly between geological sections. Despite this, the existing ichnological data revealed variations in the severity, duration and frequency of deoxygenation and can add considerable value to palaeoenvironmental interpretations determined from geochemical analyses and body fossil records.

Late Pliensbachian–earliest Toarcian. Geochemical proxies for palaeoredox (Pearce *et al.* 2008), and a reduction in the diameters of pyrite framboids (Wignall *et al.* 2005) and the abundance of calcium carbonate nodules with pyrite rims (Morris 1979), have been interpreted to indicate that reducing conditions in the Cleveland Basin were established in the *semicelatum* Subzone. However, details of the pattern and timing of the palaeoecological and palaeoenvironmental changes preceding the OAE have not yet been determined. Data from the present study shows how the benthos responded to changing conditions on Pliensbachian–Toarcian seafloors. It was comprised of several stages:

- A shift from oxygenated mostly fine-grained sediments mixed to 5 cm or more depth in the *apyrenum* Subzone to fewer ichnotaxa, and so burrow morphologies, in the lower *hawskerense* Subzone, but with a greater proportion of deeper burrowers (5–10 cm). The body fossil assemblage was diverse with a range of taxonomic groups present (Caswell *et al.* 2009; Caswell and Frid 2017). In the upper *hawskerense* Subzone, the intensity of bioturbation, ichnotaxa diversity, body fossil diversity and tracemaker body-size increased, and became highly variable near the stage boundary. Tracemakers ranged in size from millimetric *Chondrites* and *Phycosiphon* up to 60 mm *Thalassinoides*. More suspension/filter feeding trace-makers occurred, the proportions of shallow and deep burrowers were similar, and the nature of bioturbation switched from predominantly biodiffusive mixing to include more regeneration, vertical conveyance and gallery biodiffusion. The macrofaunal communities of the *apyrenum* and *hawskerense* subzones are typical of normal benthic assemblages suggesting it was oxygenated for much of the time. This

interpretation is consistent with palaeoxygenation models interpreted from trace fossil diversity, size and burrowing depth (Savrda and Bottjer 1986) and interpretations from benthic assemblages in modern deoxygenated environments (e.g., Pearson and Rosenberg 1978; Caswell *et al.* 2018).

- The Pliensbachian–Toarcian stage boundary can be distinguished by a drop in bioturbation, across a finely laminated shale (known as the Sulfur Band). In places these shales are penetrated by organisms burrowing down from above (Fig. 3D–F). Shifts in ichnodiversity, burrow orientation, ichnofabric index and tracemaker body-size across the Pliensbachian–Toarcian boundary correspond with elevated organic carbon content and a -1 to -2 ‰ $\delta^{13}\text{C}$ shift (recorded in marine and terrestrial organic matter; Littler *et al.* 2010) in the Cleveland Basin and mass extinction of marine benthic and pelagic taxa just above the stage boundary (based on body fossils (ii), Fig. 5; Caswell *et al.* 2009) across the Boreal, Tethyan and Panthalassa oceans. This coincides with negative C-isotope shifts in other NW Tethys and the Panthalassa Ocean sections at this time (e.g., Hesselbo *et al.* 2007; Caswell *et al.* 2009; Al-Suwaidi *et al.* 2010; Hesselbo and Pienkowski 2011; Xu *et al.* 2018; Them *et al.* 2019). There is also evidence for deoxygenated seafloors (from Thallium isotopes) at the stage boundary in other sections, in the SW German Basin and western Canadian Basin; Them *et al.* 2019), and this coincides with the disappearance of trace fossils at the stage boundary in the western Canadian Basin (Martindale and Aberhan 2017).
- Above the stage boundary bioturbation and ichnodiversity were initially high but very variable suggesting stressed and unstable benthic communities. Laminated organic rich horizons occur in both the lower *paltum* and *clevelandicum* subzones and correspond with organic enrichment of 2–4% TOC (Littler *et al.* 2010)(Fig. 1). The laminated organic rich horizons of *paltum*–*clevelandicum* Subzone age that occur in the Cleveland Basin are also found in SW and NW Germany (Savrda and Bottjer 1989; Röhl and Schmid-Röhl 2005; Galasso *et al.* 2021). By the middle of the *paltum* Subzone bioturbation had decreased, fewer different trace fossil morphologies occurred, tracemakers were much smaller and sediments were mixed to shallower depths. This assemblage is typical of deoxygenated ichnocoenoses ORI2 of Savrda

and Bottjer (1986) which has 2–4 ichnotaxa (of ≤ 6 mm diameter) that penetrate sediments to 2–4 cm depth.

- In the *clevelandicum*–*tenuicostatum* subzones bioturbation drops to zero (over a 4–5 m interval) as sediments become uninhabitable, this is punctuated by two macroinfaunal recolonisation events with occasional *Ophiomorpha*, *Rhizocorallium* and *Planolites*, suggesting brief oxygenation. The *Ophiomorpha* from this interval were all pyritised, abundant pyritised burrows are also observed in the *paltum* (this study) and *semicelatum* subzones at Kettlecess (Wignall *et al.* 2005). The trace fossil assemblage is typical of the lowest oxygen ichnocoenoses proposed by Savrda and Bottjer (1986) ranging from: ORI1 with 1–2 ichnotaxa (usually *Chondrites* and *Planolites*) that are ≤ 3 mm diameter and burrow sediments to ≤ 2 cm depth, to ORI2 with 2–4 ichnotaxa, ≤ 6 mm diameter burrowing to 2–4 cm depth. It is also typical of the stressed “transition zone” described for present-day benthos under organic enrichment (Pearson and Rosenberg 1978; Caswell and Frid 2017). Geochemical proxy data have been interpreted as showing a progression from oxic to regionally anoxic (Fig. 1; Pearce *et al.* 2008) trace fossil data suggest conditions were deoxygenated in the Cleveland Basin from sometime in the *paltum* Subzone.

The Oceanic Anoxic Event. Midway through the *semicelatum* Subzone trace fossils disappear, the facies change colour and become finely laminated, confirming geochemical proxy data taken to indicate that widespread deoxygenation became established at this time (Fig. 1; Pearce *et al.* 2008). From this point until the middle of the *commune* Subzone (bed 52) there is almost no evidence for macrofaunal bioturbation at any of the Yorkshire coastal outcrops or Core N1. This bioturbation gap is evident across the suite of different parameters employed, e.g. the ichnofabric index is zero, trace fossils are observed only once (*Trichichnus* sp. A occurs in bed 48 at Saltwick Bay; Fig. 4G), and almost all of the facies during this interval are laminated. The occurrence of *Trichichnus* sp. A is consistent with previous observations of the ichnogenera, e.g. that it occurs in poorly oxygenated sediments and is often the first trace fossil found after deoxygenation (Uchman 1995). For these reasons the tracemaker has previously been interpreted as having a chemosymbiotic mode of life (Uchman 1999) or being formed by sulfur-oxidising bacterial mats (Kedzierski *et al.* 2015), although the specimens found in this study seem too large to fit the latter interpretation.

Similar to the Toarcian bioturbation gap, very large defaunated areas with laminated sediments are observed in the deoxygenated parts of the Baltic Sea (Karlson *et al.* 2002; Gammal *et al.* 2017). Shallowing of sediment mixing depths (from 20 cm to a few cm only) are also demonstrated in sediment cores from hypoxic parts of the Adriatic Sea, which correspond with high organic content, more frequent seasonal hypoxia and high abundances of the opportunist bivalve *Varicorbula gibba* (Tomašových, *et al.* 2018). Unlike present-day systems where deposit feeders proliferate in deoxygenated areas (Karlson *et al.* 2002; Levin *et al.* 2009; Gogina *et al.* 2014; Caswell *et al.* 2018), deposit feeders were absent throughout the unbioturbated interval in the Toarcian when the seafloor switched to become dominated by very high abundances (Fig. 2) of monospecific suspension/filter feeding epifaunal bivalves *Bositra radiata (semicelatum* Subzone) or *Pseudomytiloides dubius (exaratum–falciferum* subzones) (Caswell and Coe 2013). A shift to epifaunal suspension feeding is observed contemporaneously in other basins (Fürsich *et al.* 2001; Röhl *et al.* 2001; Martindale and Aberhan 2017; Molina *et al.* 2018; Ros-Franch *et al.* 2019), and on other ancient deoxygenated seafloors (Savrda and Bottjer 1987; Boyer and Droser 2009).

At two notable horizons in *falciferum* Zone there is some evidence for infauna. Firstly, at the end of the negative carbon isotope excursion at the *exaratum–falciferum* zone boundary (Fig. 1) body fossils of *G. rhombifera* occur, a species with a deep infaunal life habit (Caswell *et al.* 2009), although it was not observed in living position and no trace fossils were observed suggesting it was not living infaunally at that time. Secondly, at the *falciferum–bifrons* zone boundary the infaunal brachiopod *L. longovicensis* (Caswell *et al.* 2009) and small pyritised branching trace fossils occur (Fig. 4G) suggesting brief period of oxygenation and shifting of the redox boundary below the sediment-water interface.

Palaeoenvironmental interpretations based on changes in redox sensitive elements in the Cleveland Basin have described the *falciferum–lower commune* subzones as a period of regional deoxygenation (Pearce *et al.* 2008; Fig. 1), the body (Caswell *et al.* 2009; Caswell and Dawn 2019) and trace fossil records (this study) confirm that it was not amenable to infauna. Studies of seafloor communities along an oxygenation gradient in the present-day Oman Margin Oxygen Minimum Zone showed that below 0.13–0.27 ml l⁻¹ dissolved oxygen burrowing was substantially reduced (Demaison and Moore 1980; Smith and Lyons 2013). The absence of bioturbators during these periods therefore suggests that dissolved oxygen concentrations were below 0.13 ml l⁻¹.

Similar to the Cleveland Basin, in the SW German Basin thin weakly bioturbated horizons occur near the end of the OAE (above and below the Oberer Stein), although body fossils of infaunal taxa are not reported from this horizon (Röhl *et al.* 2001; van Acken *et al.* 2019). These were interpreted as representing oxygenation events of differing duration or magnitude in an otherwise anoxic system (Savrda and Bottjer 1989). Phosphatised conservation-lagerstätten in the *falciferum* Zone of sections in SW Germany, Ilminster, UK, and Alberta, Canada are interpreted to reflect ephemeral pulses of oxygenation when the redox boundary moved below the sediment-water interface (Sinha *et al.* 2021). In the Dutch Central Graben, situated between the Cleveland and NW German basins thin bioturbated intervals suggest intermittent benthic deoxygenation (Gröcke *et al.* 2011). Conversely, in the Betic sections which are more open-ocean (Rodríguez-Tovar and Uchman 2010), the Fuente de la Vidriera and Iznalloz successions were bioturbated throughout (Reolid *et al.* 2015; Reolid *et al.* 2018), indicating an absence of benthic anoxia. Elsewhere in southern Spain in La Cerradura and Arroyo Mingarrón there was a sharp but brief decrease in early Toarcian ichnodiversity (Reolid *et al.* 2014, Šimo and Reolid 2021), and in the Fonte Coberta section, Portugal, Lusitanian Basin there was only a minor effect on tracemakers (Miguez-Salas *et al.* 2017), showing this was spatially variable. In the Umbria Marche Basin despite being closer to Tethys margin, also showed a shift from well-oxygenated facies through to laminated black shales with only occasional trace fossils (Monaco *et al.* 1994). On the north-western edge of Tethys, in hemipelagic sections of the western Carpathians, ichnodiversity decreased, and although condensed, a bioturbation gap is apparent during the OAE followed by delayed recovery of bioturbation in the *falciferum* Zone (Müller *et al.* 2020), demonstrating the importance of local hydrodynamics.

Recovery from the oceanic anoxic event. The full reappearance of infauna, as indicated by the trace fossil record, midway through the *commune* Subzone appears to be contemporaneous between the coastal exposures and those recorded in core N1. Re-establishment of the infauna after the OAE seems to have been gradual, being initially very variable. First body fossils of the infaunal deposit feeding bivalve *D. ovum* occur which dominated throughout the upper *commune* Subzone (Caswell and Dawn 2019) followed by the trace fossils ~60–120 Ka later (using the timescale of Kemp *et al.* 2011 for the Cleveland Basin) suggesting that initially *D. ovum* were not actively burrowing. Few *D. ovum* were found oriented in infaunal life-position (orthogonal to the bedding; Caswell and Dawn

2019), contrastingly in the late Pliensbachian steinkerns of the infaunal bivalve *Pholadomya* are usually found in life position. It is likely that similar to present-day facultatively infaunal bivalves, *D. ovum* live epifaunally when overlain by deoxygenated watermasses (e.g., Rosenberg and Loo 1988; Norrko and Bonsdorff 1996; Riedel et al. 2014).

The number of ichnotaxa present within any one stratigraphic horizon after the OAE (*bifrons* Zone) was at least half that during the late Pliensbachian (*spinatum* Zone), the amount of bioturbation was lower, tracemakers were half the size, and the majority were either semi-infaunal traces or penetrated the sediment < 50 mm. Bioturbation initially involved surface disturbance and indiscriminate shallow mixing by biodiffusers, by the *crassum* Subzone, although facies were often laminated, more discrete biogenic structures were being produced some of which were bioirrigated. These infaunal communities cannot be considered equivalent to the climax state of 'normal/healthy' present-day communities (Pearson and Rosenberg 1978; Gray et al. 2002; Borja et al. 2012; Dietl et al. 2016) nor those of the late Pliensbachian because they lacked a significant amount of deep burrowing. Although geochemical data are fewer from this interval, proxies for palaeoredox conditions support this interpretation with bottom water hypoxia–anoxia persisting in the *bifrons* Zone (Fig. 1, Pearce et al. 2008). Conditions for macroinfauna in the Cleveland Basin after the OAE seemed far more dynamic than during the onset to the event, e.g., the sedimentary lamination, pyrite replacement, bioturbatory mode, ichnotaxa number, size and orientation varied far more in the *bifrons* Zone than during the late Pliensbachian–earliest Toarcian. Palaeoredox proxies show that hypoxia–anoxia also persisted during the *bifrons* Zone in the western Canadian and SW German basins (Them et al. 2019).

Trace fossils of all types were found pyritised throughout the *commune*–*crassum* subzones, indicating preservation in reducing sediments with high concentrations of sulfur and iron but also that sediments were not reoxygenated post burial, because if the pyrite is reoxidised it does not preserve (Scheiber 2002; Gingras et al. 2014). Bivalves with pyritised internal linings preserved in sediment cores deposited under analogous deoxygenated present-day conditions in the northern Adriatic Sea have been interpreted as indicating restricted bioirrigation in space and time (Tomašových et al. 2021). For instance, under conditions where recovery from hypoxia is slow and benthic communities have low bioirrigation potential and mix sediments to shallow depths only (Tomašových et al. 2021). The pyritization of burrows in the lower *semicelatum* Subzone (*tenuicostatum* Zone) and throughout much of the *bifrons* Zone in the Cleveland Basin thus confirms that conditions were regionally hypoxic for prolonged periods during the *bifrons* Zone with shallow sediment redox boundaries and only weak bioirrigation. This interpretation is consistent with the

lack of body and trace fossils with deep infaunal habits. In addition to pyritised burrows, many bivalve body fossils are preserved with thin pyrite linings in the *semicelatum*–*commune* subzones of the Cleveland Basin (Caswell *et al.* 2009; Caswell & Dawn 2019) confirming that any periods of oxygenation during the deposition of these zones were short and did not mix sediments to depth (e.g., this is the case at the *exaratum*–*falciferum* Zone boundary where pyritized *Meleagrinea substriata* and *Goniomya rhombifera* occur; Caswell *et al.* 2009).

In low diversity hypoxic communities, one or two dominant species can contribute more to nutrient cycling than multiple species within a more taxonomically diverse community (Norkko *et al.* 2015), thus the behaviour of the deposit feeding bivalve *D. ovum* and the tracemakers inhabiting *bifrons* Zone seafloors may have played an important role in its recovery. The re-establishment of infauna is a fundamental step in marine ecosystem recovery, as increased bioturbation helps to reoxygenate sediments, creating biogenic habitat for taxa that are intolerant of low oxygen (e.g., Volkenborn *et al.* 2007), stimulating microbial respiration and increasing sediment-water exchange and nutrient fluxes (Mermillod-Blondin 2011). Present-day ecosystems experiencing severe short-term hypoxia can take years to recover, and where severe hypoxia lasts for longer periods (i.e., decades–centuries) recovery is even slower and hysteretic (Stachowitsch 1991; Diaz and Rosenberg 2008; Conley *et al.* 2009; Tomašových *et al.* 2018). The Toarcian recovery trajectory was protracted in restricted palaeoenvironmental settings such as the Cleveland Basin (Danise *et al.* 2013; Caswell and Frid 2017), and is even more so in NE Panthalassa (Martindale and Aberhan 2017) and in the Arctic Ocean (Suan *et al.* 2011) where there are no signs of macroinfaunal recovery in strata equivalent to the *bifrons* Zone of NW Europe.

Palaeoenvironmental drivers of changes on the seafloor. In the Cleveland Basin changes in body fossil assemblage structure were driven by local redox conditions (Caswell and Frid 2017) whereas changes in population density and body-size of the opportunistic bivalves was driven by changes in primary production (Caswell and Coe 2013). It is highly likely that palaeoredox caused the loss of infauna, declines in the diversity of infaunal behaviours present and tracemaker body size. This is consistent with present-day deoxygenation, where benthic diversity declines and the seafloor may become completely devoid of macrofauna, bioturbation shallows or ceases depending on the severity of deoxygenation (Pearson and Rosenberg 1978; Gray *et al.* 2002; Breitburg *et al.* 2018; Caswell *et al.* 2018; Tomašových *et al.* 2018). Observations from the Toarcian of the Cleveland Basin are consistent with those from present-day oxygen minimum zones, where the amount of burrowing, burrower body-size and the range of burrowing modes present decrease as oxygen declines (Smith *et al.* 2000, Tomašových *et al.* 2020). Similar observations have been made from

deoxygenated Late Devonian seafloors (Boyer and Droser 2011; Boyer *et al.* 2011), Late Cretaceous and End Permian seafloors (Savrda and Bottjer 1986; Twitchett and Barras 2004; Wiest *et al.* 2015).

The implications of Pliensbachian–Toarcian changes for ecosystem functioning

The changes observed in response to deoxygenation in the Toarcian are consistent with the biological changes induced by present-day deoxygenation, biodiversity and productivity are impacted, trophic structure changes, bioturbation declines or ceases and there is extensive habitat loss (Pearson and Rosenberg 1978; Gray *et al.* 2002; Breitburg *et al.* 2018). Few studies of deoxygenation span decadal or longer timescales (however, see Borja *et al.* 2006; Carstensen *et al.* 2014; Gogina *et al.* 2014; Norkko *et al.* 2015; Hale *et al.* 2016, Tomašových *et al.* 2020), but if we wish to understand the impacts of these changes for ecosystem functioning we need to look at change over longer timescales and larger spatial scales (Thrush *et al.* 2013; Norkko *et al.* 2015; Breitburg *et al.* 2018). Especially because ecosystems experiencing severe deoxygenation are unpredictable and can take decades to recover (Stachowitsch 1991; Diaz and Rosenberg 2008; Conley *et al.* 2009; Tomašových *et al.* 2018). Furthermore, the impacts on ecosystem-wide functioning take time to manifest, e.g. changes in biogeochemical cycling (Jessen *et al.* 2017) and effects higher in the food chain (Casini *et al.* 2016). Marine ecosystem functioning is strongly coupled with benthic processes that oxygenate sediments, determine secondary production, drive the biogeochemical cycling of organic carbon and nutrients (Snelgrove 1997; Costello *et al.* 2015), which alter food web dynamics. Thus, the major shifts in macrofaunal behaviour that occurred during the Toarcian OAE would have profoundly affected ecological functioning.

Nutrient cycling and regeneration. Bioturbation is a critical driver of biogeochemical processes in areas such as the Cleveland Basin where sediments are predominantly fine grained (sandy–muddy) and hydrological exchange between interstitial waters and the overlying water column is primarily determined by diffusion (Mermillod-Blondin 2011). Sediment oxygenation and aerobic microbial respiration rates are faster when sediment mixing rates, burrowing depths and burrow complexity are higher. For instance, the presence of U-shaped burrows and subsurface galleries can increase sediment microbial respiration by 250% (Karlson *et al.* 2005), and deep bioirrigated galleries can increase sediment–water fluxes by 2000% (Rasmussen *et al.* 1998). In turn, these processes determine the fluxes of sedimentary nitrogen and mineralization products into the water column (Kristensen and Blackburn 1987; Hansen and Blackburn 1992; Lohrer *et al.* 2004) and so are critical drivers of ocean nutrient and carbon cycling (Fitch and Crowe 2011;

Snelgrove *et al.* 2018; Aller and Cochran 2019; Solan *et al.* 2020). In the late Pliensbachian-early Toarcian the amount of bioturbation, burrowing depth, the bioturbatory modes employed, and the size of biogenic constructs varied considerably.

The switch from predominantly biodiffusive mixing in the *apyrenum* Subzone to more regeneration, upward and downward conveyance and gallery biodiffusion, and the increased mixing depths in the *hawskerense* and lower *paltum* subzones should correspond with increased sediment-water exchange, sediment oxygenation and the creation of sediment biogeochemical gradients. The net result of these changes would likely have been increased sedimentary fluxes of nitrates in to the water column stimulating primary productivity (Jørgensen *et al.* 1995; Graf and Rosenberg 1997; Kristensen 2000). Above the stage boundary, reductions in the amount of bioturbation, mixing depths and the range of bioturbatory modes expressed, will have reduced the macrobenthic contributions to sediment oxygenation, hydrological exchange and biogeochemical cycling (Snelgrove 1997; Costello *et al.* 2015).

The lack of macroscopic trace fossils for much of the *clevelandicum*–*semicelatum* subzones (*tenuicostatum* Zone) and all of the *falciferum*–lower *bifrons* zones suggests that bioturbation ceased completely. The astronomical timescales suggest that this “bioturbation gap” lasted for between 0.6 and 2.5 Ma in the Cleveland Basin (if constant sedimentation rates are assumed; Suan *et al.* 2008; Kemp *et al.* 2011; Suan *et al.* 2011). Bioturbation gaps of differing durations have also been observed from several other Toarcian sections in the NW Tethys, e.g. NW German and SW German basins (Savrda and Bottjer 1989; Röhl *et al.* 2001; Röhl and Schmid-Röhl 2005), Dutch Central Graben (Trabucho-Alexandre *et al.* 2012), North Gondwanan palaeomargin (Ruebsam *et al.* 2020a; Reolid *et al.* 2021b); Northern Iberian Margin (Fernández-Martínez *et al.* 2021); Panthalassa Ocean sections in Alberta, Canada (Martindale and Aberhan 2017); and the Arctic Basin, N Siberia (Suan *et al.* 2011). In the Western Canadian and Arctic basins, similar to the Cleveland Basin, macroscopic trace fossils were absent for much longer (*tenuicostatum*–lower *bifrons* zones). The collapse of bioturbation over large parts of the continental shelf in the northern hemisphere (documented for the NW Tethys, NE Panthalassa and Boreal Ocean) during the Toarcian would have driven regional-scale changes in biogeochemical cycling. For instance, present-day macrofaunal communities and benthic nutrient fluxes, covary by several orders of magnitude along oxygen gradients across the Baltic Sea (Norkko *et al.* 2015). Large

defaunated areas have at times covered approximately one quarter of the Baltic seafloor, these sediments are laminated and lack bioturbators (Karlson *et al.* 2002; Gammal *et al.* 2017) as observed in the Cleveland Basin (upper *semicelatum*-mid *commune* subzones). The dynamics of the biogeochemical cycling change under hypoxia, with increased phosphate and ammonia fluxes (Jørgensen *et al.* 1995; Hale *et al.* 2016). The additional phosphate can cause negative feedbacks by stimulating further primary production and deoxygenation (Jørgensen *et al.* 1995). The exceptional preservation of marine fossil lagerstätten in the UK, Canada and SW Germany by phosphatisation show that phosphate availability increased during the OAE partly due to its release from anoxic sediments (Sinha *et al.* 2021).

Food web dynamics. Seafloor palaeocommunities were dominated by 2–3 species only throughout the *falciferum* Zone, for example in the Cleveland Basin, Paris Basin and SW and NW German basins, western Canadian Basin, Arctic Basin and the Neuquen Basin (Riegraf 1982; Fürsich *et al.* 2001; Röhl *et al.* 2001; Caswell and Coe 2013; Martindale and Aberhan 2017; Ros-Franch *et al.* 2019). In most cases the dominant species were epifaunal suspension feeding bivalves or brachiopods, and many underwent large changes in body size during the OAE (Caswell and Coe 2013; Comas-Rengifo *et al.* 2015; Piazza *et al.* 2019; Piazza *et al.* 2020; Ros-Franch *et al.* 2019). The shifts from a predominantly deposit feeding benthos towards an almost exclusively suspension feeding epifauna in many areas during the OAE, would have resulted in changes in organic carbon-cycling. More pelagic carbon is processed by a predominantly suspension feeding benthos (Rosenberg 1977; Pearson and Rosenberg 1978) strengthening benthic-pelagic coupling. Contrastingly, during intervals when macrofossils disappeared completely in the Cleveland Basin (e.g. Caswell and Coe 2013), anaerobic bacteria probably proliferated weakening benthic-pelagic coupling and shortening food chains when organic carbon was remineralised and reused (as shown by Rosenberg (1977) and Baird *et al.* (2004)).

There is good evidence that the Toarcian palaeoecological changes affected organisms across trophic levels in the Cleveland Basin and other areas. Extinction of benthic and pelagic marine invertebrates occurred across the Boreal, Tethys and Panthalassa oceans at both the stage boundary and just before the OAE (Little and Benton 1995; Vörös 2002; Cecca and Macchioni 2004; Ruban 2004; Zakharov *et al.* 2006; Caswell *et al.* 2009; Caruthers

et al. 2013). In addition to the changes in benthic macrofauna, the composition of benthic meiofauna (e.g., Nikitenko *et al.* 2013; Reolid *et al.* 2012; Rita *et al.* 2016), phytoplankton and zooplankton assemblages changed across the NW Tethys, and so did the size and morphology of selected taxa groups (e.g., Palliani and Riding 1999; Palliani *et al.* 2002; Schwark and Frimmel 2004; van Breugel *et al.* 2006; Hermoso *et al.* 2009; Van de Schootbrugge *et al.* 2013; Reolid *et al.* 2014; Clemence *et al.* 2015; Correia *et al.* 2017; Galasso *et al.* 2021; Reolid and Ainsworth 2022; Reolid *et al.* 2019). Showing that both primary and secondary production changed over this period. Changes in the biogeographic distribution of marine nekton including ammonites (Dera *et al.* 2011) and belemnites, and changes in the body size of the latter are also apparent in NW Tethys (Caswell and Coe 2014; Rita *et al.* 2018; Rita *et al.* 2019). Changes in the size of predators such as ichthyosaurs have been linked with changes in their diet (Maxwell and Vincent 2016) showing the influence of changes at lower trophic levels. Although more evidence is needed on the changes at higher trophic levels across the late Pliensbachian-early Toarcian, changes in primary and secondary production, and trophic connections show that marine ecosystem functioning did change at least regionally.

The Pliensbachian–Toarcian trace fossil record of seafloor change: integrated data sources

Palaeoenvironmental change is often documented from body and trace fossil records separately, but when used together they offer far greater power because trace fossils are often the only record of taxa with low preservation potential. Direct comparison of high resolution geochemical and palaeontological records by Boyer and Droser (2011) showed that they revealed complementary information. With geochemistry being useful for distinguishing anoxia from euxinia and describing the prevailing palaeoenvironmental conditions; where, palaeontological data provide more information on the progression from hypoxia through to anoxia, fluctuations in oxygenation and the biological consequences. Although geochemical data are lacking for some important intervals in the NE Yorkshire section (Fig. 1), we also found that the geochemical data from Yorkshire described the broad palaeoenvironmental changes, but did not capture detailed changes on the seafloor such as the development and timing of deoxygenation, brief periods of reoxygenation. Nor did it capture fluctuations in the position of the redox boundary across the sediment-water interface (e.g., as reflected by the preservation of pyritised fossils) nor within the sediments

(e.g. that corresponded with changes in burrowing depth, body fossils of infauna). Specific observations include:

- Changes in trace fossils across the Pliensbachian–Toarcian stage boundary corresponded with palaeoenvironmental changes (from geochemistry) and mass extinction horizon (ii)
- Palaeontological data agreed that deoxygenation began in the *tenuicostatum* Zone, but changes in sedimentary lamination, ichnofabric index, ichnotaxon number, size and functional traits revealed the point at which conditions shifted from being predominantly oxygenated to deoxygenated occurred in the mid *paltum* Subzone (Figs 5-6).
- Show that bioturbation, ichnodiversity and burrow size were initially high but very variable above the stage boundary and once infauna reappeared in the mid-*commune* Subzone suggesting the macroinfauna were unstable and stressed.
- Several periods of brief reoxygenation are shown for the *clevelandicum*–*tenuicostatum* subzones, the *exaratum*–*falciferum* and *falciferum*–*bifrons* subzone boundaries (Fig. 5).
- Geochemical evidence has been interpreted to indicate that global changes in ocean deoxygenation were established in the upper *semicelatum* Subzone in Yorkshire but this may have occurred earlier in the subzone before or after the last tracemaker (pyritised *?Ophiomorpha*) disappeared (Fig. 5).
- Sedimentary lamination and a lack of trace fossils confirm geochemical interpretations that conditions continued to be regionally hypoxic during the *bifrons* Zone, but they show that this changed in the mid-*commune* Subzone (Fig. 5). Where trace fossil preservation as pyrite, intermittent sedimentary lamination, small tracemaker body size and the lack of body or trace fossils with deep infaunal habits showed that deoxygenation continued until at least the *crassum* Subzone (Figs 5-6) with shallow sediment redox boundaries and only weak bioirrigation.

In terms of the broad palaeoenvironmental trends observed, good agreement was found between the timing and nature of changes in trace fossil assemblages (ichnodiversity, ichnofabric index and ichnometrics) from the core and coastal outcrops, although the stratigraphic resolution of the two differed. Sedimentary laminae spanned a greater

stratigraphic range in the core, and overall the core contained fewer ichnotaxa, they were generally smaller (up to 20 mm) and less were vertically oriented compared to the coastal exposures. These differences probably reflect the greater visibility of fine details and inability of core to capture some larger trace fossils. At outcrop preservational factors can make trace fossils more or less obvious, for example trace fossils are preserved with greater relief in some of the siderite nodules (Fig. 3A–B) or when pyritised (Fig. 4D), and they are more subtle, e. g. the *Palaeophycus* in bed 52 (Fig. 4F) where the trace fossil fill is similar to the matrix. This may have led to some under-representation of the trace fossil assemblage, and so the use of independent metrics (e.g., the ichnofabric index, sedimentary lamination, as well as ichnotaxa) and cross-verification with changes in the core are important.

Conclusions

Changes in Toarcian marine ecosystems share many similarities with the present-day and other palaeoenvironmental events, specifically those experiencing deoxygenation. Changes on the seafloor fit with predictions that species extinctions in the oceans today will lead to declines in bioturbation (Solan *et al.* 2004). The scale of this change is expected to correspond with the biological traits of the species lost, and so exploring changes in ecological functioning from past ecosystems experiencing extreme change can help us to understand these dynamics.

Often the only demonstrably *in situ* features of marine successions trace fossils can show how the palaeoenvironment changed, and so can bridge interpretations from geochemical proxies and body fossils. Integration of high resolution lithological, geochemical, body fossil and trace fossil records can improve interpretations of palaeoenvironmental and palaeoecological change. The detailed trace fossil data presented in this study, reveal new details about the pattern of deoxygenation in the Cleveland Basin prior to and after the OAE where geochemical data are fewer. It also contributes to our understanding of how the benthos as a whole were impacted (trace and body fossils) and recolonised in the aftermath. It also allows consideration of the implications of these changes for marine ecosystem structure and functioning. For instance, changes in biogeochemical cycling, primary and secondary production and food-web dynamics during the Toarcian.

Detailed palaeontological investigation of some of the more “minor” periods of ancient marine ecosystem change (i.e., not the big five mass extinctions), can provide analogues that contribute to our understanding of the responses of ecosystem dynamics and functioning to near-future

environmental change. For instance, by helping to define thresholds for change, and understanding what the longer-term and larger scale ecological impacts of the present-day changes might be.

Acknowledgments

Facilities were provided by the School of Environment, University of Hull, School of Environment, Griffith University. Thanks to Anglo American (previously Sirius Minerals) for facilitating access to Doves Nest core N1. Thanks to the editorial team for co-ordinating the special issue, Adam Tomašových, Mattias Reolid and one anonymous reviewer for constructive feedback has helped to improve the work. Thanks to João Trabucho-Alexandre, Elizabeth Atar, Steve Livera, Peter Rawson, Duncan McIlroy, Angela Coe, Chris Frid, David Bond for discussions that helped to develop the work. Steve Livera, Angela Coe, Eleanor Maddison, Patricia Clay, Alison Hunt, David Wetherby, Anthony Cohen, Peter Sheldon, Stephanie Dawn, Paul Scott, and Alice Kennedy for help with fieldwork. Discussions within the Working Group on the History of Fish and Fisheries (WGHIST) of the International Council for the Exploration of the Sea (ICES) have helped to inspire elements of this work. New data from this study will be made available after a period of embargo, but if interested in this data in the mean-time please contact the corresponding author.

References

- Al-Suwaidi, A.H., Angelozzi, G.N. *et al.* 2010. First record of the Early Toarcian Oceanic Anoxic Event from the Southern Hemisphere, Neuquén Basin, Argentina. *Journal of the Geological Society, London*, **167**, 633–636, <https://doi.org/10.1144/0016-76492010-025>.
- Aller, R.C. and Cochran, J.K. 2019. The critical role of bioturbation for particle dynamics, priming potential, and organic C remineralization in marine sediments: local and basin scales. *Frontiers in Earth Science*, **7**, 157.
- Bailey, T.R., Rosenthal, Y., McArthur, J.M., van de Schootbrugge, B. and Thirlwall, M.F. 2003. Paleoceanographic changes of the Late Pliensbachian–Early Toarcian interval: a possible link to the genesis of an Oceanic Anoxic Event. *Earth and Planetary Science Letters*, **212**, 307–320.
- Baird, D., Christian, R.R., Peterson, C.H. and Johnson, G.A. 2004. Consequences of hypoxia on estuarine ecosystem function energy diversion from consumers to microbes. *Ecological Applications*, **14**, 805–822.
- Bambach, R.K., Bush, A.M. and Erwin, D.H. 2007. Autecology and the filling of ecospace: Key metazoan radiations. *Palaeontology*, **50**, 1–22.
- Bertling, M. 2011. What's in a name? Nomenclature, systematics, ichnotaxonomy. *In*: Miller, W.I. (ed.) *Trace fossils: concepts, problems and prospects*. Elsevier, Oxford, 81–91.
- Bolam, S.G. and Eggleton, J.D. 2014. Macrofaunal production and biological traits: spatial relationships along the UK continental shelf. *Journal of Sea Research*, **88**, 47–58, <https://doi.org/10.1016/J.SEARES.2014.01.001>.
- Borja, Á., Muxika, I. and Franco, J. 2006. Long-term recovery of soft-bottom benthos following urban and industrial sewage treatment in the Nervión estuary (southern Bay of Biscay). *Marine Ecology Progress Series*, **43**, 43–55.
- Borja, Á., Dauer, D.M. and Grémare, A. 2012. The importance of setting targets and reference conditions in assessing marine ecosystem quality. *Ecological Indicators*, **12**, 1–7.
- Boyer, D.L. and Droser, M.L. 2009. Palaeoecological patterns within the dysaerobic biofacies: Examples from Devonian black shales of New York state. *Palaeogeography, Palaeoclimatology, Palaeoecology*, **276**, 206–216.

Boyer, D.L. and Droser, M.L. 2011. A combined trace- and body-fossil approach reveals high-resolution record of oxygen fluctuations in Devonian seas. *Palaios*, **26**, 500–508.

Boyer, D.L., Owens, J.D., Lyons, T.W. and Droser, M.L. 2011. Joining forces: Combined biological and geochemical proxies reveal a complex but refined high-resolution palaeo-oxygen history in Devonian epeiric seas. *Palaeogeography, Palaeoclimatology, Palaeoecology*, **306**, 134–146.

Breitburg, D., Levin, L.A. *et al.* 2018. Declining oxygen in the global ocean and coastal waters. *Science*, **359**, 1–13.

Bremner, J., Rogers, S.I. and Frid, C.L.J. 2006. Methods for describing ecological functioning of marine benthic assemblages using biological traits analysis (BTA). *Ecological Indicators*, **6**, 609–622.

Bulling, M.T., Hicks, N., Paterson, D.M., Raffaelli, D.G., White, P.C.L. and Solan, M. 2010. Marine biodiversity–ecosystem functions under uncertain environmental futures. *Philosophical Transactions - Royal Society of London, B*, **365**, 2107–2116, <https://doi.org/10.1098/rstb.2010.0022>.

Caliman, A., Leal, J.J.F., Esteves, F.A., Carneiro, L.S., Bozelli, R.L. and Farjalla, V.F. 2007. Functional bioturbator diversity enhances benthic-pelagic processes and properties in experimental microcosms. *Journal of the North American Benthological Society*, **26**, 450–459, <https://doi.org/10.1899/06-050.1>.

Carstensen, J., Conley, D.J. *et al.* 2014. Hypoxia in the Baltic Sea: Biogeochemical Cycles, Benthic Fauna, and Management. *Ambio*, **43**, 26–36.

Caruthers, A.H., Gröcke, D.R. and Smith, P.L. 2011. The significance of an Early Jurassic (Toarcian) carbon-isotope excursion in Haida Gwaii (Queen Charlotte Islands), British Columbia, Canada. *Earth & Planetary Science Letters*, **307**, 19–26, <https://doi.org/10.1016/j.epsl.2011.04.013>.

Caruthers, A.H., Smith, P.L. and Grocke, D.R. 2013. The Pliensbachian–Toarcian (Early Jurassic) extinction, a global multi-phased event. *Palaeogeography, Palaeoclimatology, Palaeoecology*, **386**, 104–118.

Casini, M., Käll, F. *et al.* 2016. Hypoxic areas, density-dependence and food limitation drive the body condition of a heavily exploited marine fish predator. *Royal Society Open Science*, **3**, 160416.

Caswell, B.A. 2010. *The response of the marine biota to the early Toarcian (Early Jurassic) oceanic anoxic event*. PhD, The Open University.

Caswell, B.A. and Coe, A.L. 2013. Primary productivity controls on opportunistic bivalves during Early Jurassic oceanic anoxia. *Geology*, **41**, 1163–1166, <https://doi.org/10.1130/G34819.1>.

Caswell, B.A. and Coe, A.L. 2014. The impact of anoxia on pelagic macrofauna during the Toarcian Oceanic Anoxic Event (Early Jurassic). *Proceedings of the Geologists' Association*, **125**, 383–391, <https://doi.org/http://dx.doi.org/10.1016/j.pgeola.2014.06.001>.

Caswell, B.A. and Frid, C.L.J. 2017. Marine ecosystem resilience during extreme deoxygenation: the Early Jurassic oceanic anoxic event. *Oecologia*, **183**, 275–290, <https://doi.org/10.1007/s00442-016-3747-6>.

Caswell, B.A. and Dawn, S.J. 2019. Recovery of benthic communities following the Toarcian oceanic anoxic event in the Cleveland Basin, UK. *Palaeogeography, Palaeoclimatology, Palaeoecology*, **521**, 114–126.

Caswell, B.A., Coe, A.L. and Cohen, A.S. 2009. New range data for marine invertebrate species across the early Toarcian (Early Jurassic) mass extinction. *Journal of the Geological Society, London*, **166**, 859–872.

Caswell, B.A., Paine, M. and Frid, C.L.J. 2018. Seafloor ecological functioning over two decades of organic enrichment. *Marine Pollution Bulletin*, **136**, 212–229.

Cecca, F. and Macchioni, F. 2004. The two Early Toarcian (Early Jurassic) extinction events in ammonoids. *Lethaia*, **37**, 35–56.

Cheung, W.W.L., Sarmiento, J.L. *et al.* 2013. Shrinking of fishes exacerbates impacts of global ocean changes on marine ecosystems. *Nature Climate Change*, **3**, 254–258, <https://doi.org/10.1038/nclimate1691>.

Chevone, F., Doleddec, S. and Chessel, D. 1994. A fuzzy coding approach for the analysis of long-term ecological data. *Freshwater Biology*, **31**, 295–309.

Clemence, M.-E., Gardin, S. and Bartolini, A. 2015. New insights in the pattern and timing of the Early Jurassic calcareous nannofossil crisis. *Palaeogeography Palaeoclimatology Palaeoecology*, **427**, 100–108.

Cohen, A.S., Coe, A.L., Harding, S.M. and Schwark, L. 2004. Osmium isotope evidence for the regulation of atmospheric CO₂ by continental weathering. *Geology*, **32**, 157–160, <https://doi.org/doi:10.1130/G20158.1>.

Comas-Rengifo, M.J., Duarte, L.V., Félix, F.F., Garcia Joral, F., Goy, A. and Rocha, R.B. 2015. Latest Pliensbachian –Early Toarcian brachiopod assemblages from the Peniche section (Portugal) and their correlation. *Episodes*, **38**, 2–8.

Conley, D.J., Carstensen, J., Vaquer-Sunyer, R. and Duarte, C.M. 2009. Ecosystem thresholds with hypoxia. *Hydrobiologia*, **629**, 21–29, <https://doi.org/10.1007/s10750-009-9764-2>.

Correia, V.F., Riding, J.B., Duarte, L.V., Fernandes, P. and Pereira, Z. 2017. The palynological response to the Toarcian Oceanic Anoxic Event (Early Jurassic) at Peniche, western Portugal. *Marine Micropaleontology*, **137**, 46–63.

Costello, M.J., Vanhooime, B. and Appelthans, W. 2015. Progressing conservation of biodiversity through taxonomy, data publication and collaborative infrastructures. *Conservation Biology*, **29**, 1094–1099.

Danise, S., Twitchett, R.J., Little, C.T.S. and Clemence, M.-E. 2013. The Impact of Global Warming and Anoxia on Marine Benthic Community Dynamics: an Example from the Toarcian (Early Jurassic). *Plos One*, **8**, e56255, <https://doi.org/10.1371/journal.pone.0056255>.

Dashtgard, S.E. and Gingras, S.E. 2012. Chapter 10: Marine Invertebrate Neoichnology. In: Knaust, D. and Bromley, R.G. (eds) *Developments in Sedimentology*. Elsevier, The Netherlands, 273–295.

Demaison, G.J. and Moore, G.T. 1980. Anoxic environments and oil source bed genesis. *American Association of Petroleum Geologists Bulletin*, **64**, 1179–1209.

Dera, G., Niege, P., Dommergues, J.-L. and Brayard, A. 2011. Ammonite palaeobiogeography during the Pliensbachian -Toarcian crisis (Early Jurassic) reflecting the palaeoclimate, eustasy, and extinctions. *Global Planetary Change*, **78**, 92–105.

Diaz, R.J. and Rosenberg, R. 2008. Spreading dead zones and consequences for marine ecosystems. *Science*, **321**, 926–929, <https://doi.org/10.1126/science.1156401>.

Dietl, G.P., Durham, S.R., Smith, J.A. and Tweitmann, A. 2016. Mollusk assemblages as records of past and present ecological status. *Frontiers in Marine Science*, **3**, 169.

Douglas, E.J., Pilditch, C.A., Kraan, C., Schipper, L.A., Lohrer, A.M. and Thrush, S. 2017. Macrofaunal Functional Diversity Provides Resilience to Nutrient Enrichment in Coastal Sediments. *Ecosystems*, **20**, 1324–1336, <https://doi.org/10.1007/s10021-017-0113-4>.

Droser, M.L. and Bottjer, D.J. 1986. A semiquantitative field classification of ichnofabric. *Journal of Sedimentary Research*, **56**, 558–559.

Ekdale, A.A. and De Gibert, J.M. 2010. Palaeoethologic significance of bioglyphs: Fingerprints of the subterraneans. *Palaios*, **25**, 540–545.

Fenchel, T. 1996. Worm burrows and oxic microniches in marine sediments. 1. Spatial and temporal scales. *Marine Biology*, **127**, 289–295.

Fenchel, T. and Finlay, B. 2008. Oxygen and the spatial structure of microbial communities. *Biological Reviews*, **83**, 553–569.

Fernández-Martínez, J., Rodríguez-Tovar, F.J., Piñuela, L., Martínez-Ruiz, F. and García-Ramos, J.C. 2021. Bottom- and pore-water oxygenation during the early Toarcian Oceanic Anoxic Event (T-OAE) in the Asturian Basin (N Spain): Ichnological information to improve facies analysis. *Sedimentary Geology*, **419**, 105909.

Fitch, J.E. and Crowe, T.P. 2011. Combined effects of temperature, inorganic nutrients and organic matter on ecosystem processes in intertidal sediments. *Journal of Experimental Biology and Ecology*, **400**, 257–263.

Francois, F., Poggiale, J.-C., Durbec, J.-P. and Stora, G. 1997. A new approach for the modelling of sediment reworking induced by a macrobenthic community. *Acta Biotheoretica*, **45**, 295–319.

Francois, F., Gerino, M., Stora, G., Durbec, J.-P. and Poggiale, J.-C. 2002. A functional approach to sediment reworking by gallery-forming macrobenthic organisms: modelling and application with the polychaete *Nereis diversicolor*. *Marine Ecology Progress Series*, **229**, 127–136.

Frey, R. W. 1970. Trace fossils of Fort Hays Limestone Member of Niobrara Chalk (Upper Cretaceous), West-Central Kansas, The University of Kansas, *Paleontological Contributions*, **53**, 1–41.

Frey, R.W., Howard, J.D. and Pryor, W.A. 1978. Ophiomorpha: Its morphologic, taxonomic, and environmental significance. *Palaeogeography Palaeoclimatology Palaeoecology*, **23**, 199–229.

Fürsich, F.T. 1974. On *Diplocraterion* Torell 1870 and the significance of morphological features in vertical spreitenbearing, U-shaped trace fossils. *Journal of Paleontology* **48**, 952–962.

Fürsich, F.T., Berndt, R., Scheuer, T. and Gahr, M. 2001. Comparative ecological analysis of Toarcian (Lower Jurassic) benthic faunas from southern France and east-central Spain. *Lethaia*, **34**, 169–199.

Galasso, F., Schmid-Röhl, A., Feist-Burkhardt, S., Bernasconi, S.M. and Schneebeil-Hermann, E. 2021. Changes in organic matter composition during the Toarcian Oceanic Anoxic Event (T-OAE) in the Posidonia Shale Formation from Dormettingen (SW-Germany). *Palaeogeography, Palaeoclimatology, Palaeoecology*, **569**, 110327.

Gammal, J., Norkko, J., Pilditch, C.A. and Norkko, A. 2017. Coastal hypoxia and the importance of benthic macrofauna communities for ecosystem functioning. *Estuaries and Coasts* **40**, 457–468, <https://doi.org/10.1007/s12237-016-0152-7>.

Gingras, M.K., MacEachern, J.A. and Dashtgard, S.E. 2011. Process ichnology and the elucidation of physico-chemical stress. *Sedimentary Geology*, **237**, 115–134.

Gingras, M.K., Dahstgard, S.E., MacEahern, J.A. and Pemberton, S.G. 2008. Biology of shallow marine ichnology: a modern perspective. *Aquatic Biology*, **2**, 255–268

Gingras, M. K., Zonneveld, J. P., and Konhauser, K. O. 2014. Using X- ray radiography to observe Fe distributions in bioturbated sediment. *In: Hembree, D.I., Platt, B.F., and Smith, J.J. (eds) Experimental Approaches to Understanding Fossil Organisms*. Springer, Dordrecht, 195–206.

Gogina, M., Darr, A. and Zettler, M.L. 2014. Approach to assess consequences of hypoxia disturbance events for benthic ecosystem functioning. *Journal of Marine Systems* **129**, 203–213.

Graf, G. and Rosenberg, R. 1997. Bioresuspension and biodeposition: A review. *Journal of Marine Systems*, **11**, 269–278.

Gray, J.S., Wu, R.S.S. and Or, Y.Y. 2002. Effects of hypoxia and organic enrichment on the coastal marine ecosystem. *Marine Ecology Progress Series*, **238**, 249–279, <https://doi.org/10.3354/meps238249>.

Gröcke, D., Hori, R.S., Trabucho-Alexandre, J. and Kemp, D.B. 2011. An open ocean record of the Toarcian oceanic anoxic event. *Solid Earth*, **2**, 247–257, <https://doi.org/10.5194/se-2-245-2011>.

Hale, S.S., Cicchetti, G. and Deacutis, C.F. 2016. Eutrophication and hypoxia diminish ecosystem functions of benthic communities in a New England estuary. *Frontiers in Marine Science*, **3**, 1–14.

Hansen, L.S. and Blackburn, T.H. 1992. Mineralization budgets in sediment microcosms: effect of the infauna and anoxic conditions. *FEMS microbiology ecology*, **11**, 33–43.

Harding, S.M. 2004. *The Toarcian oceanic anoxic event: organic and inorganic geochemical anomalies in organic-carbon-rich mudrocks from the North Yorkshire Coast, UK and Dotternhausen Quarry, SW Germany*. PhD thesis, The Open University.

Hattam, C., Atkins, J.P. *et al.* 2015. Marine ecosystem services: Linking indicators to their classification. *Ecological Indicators*, **49**, 61–75, <https://doi.org/10.1016/j.ecolind.2014.09.026>.

Hermoso, M., Le Callonnec, L., Minoletti, F., Renard, M. and Hesselbo, S.P. 2009. Expression of the Early Toarcian negative carbon-isotope excursion in separated carbonate microfractions (Jurassic, Paris Basin). *Earth and Planetary Science Letters*, **277**, 194–203, <https://doi.org/10.1016/j.epsl.2008.10.013>.

Herringshaw, L.G., Callow, R.H.T. and McIlroy, D. 2017. Engineering the Cambrian explosion: the earliest bioturbators as ecosystem engineers. *Geological Society London, Special Publications*, **448**, 369–382, doi:10.1144/SP448.18.

Hesselbo, S.P. and Pienkowski, G. 2011. Stepwise atmospheric carbon-isotope excursion during the Toarcian Oceanic Anoxic Event (Early Jurassic, Polish Basin). *Earth and Planetary Science Letters*, **301**, 365–372, <https://doi.org/10.1016/j.epsl.2010.11.021>.

Hesselbo, S.P., Jenkyns, H.C., Duarte, L.V. and Oliveira, L.C.V. 2007. Carbon-isotope record of the Early Jurassic (Toarcian) Oceanic Anoxic Event from fossil wood and marine carbonate (Lusitanian Basin, Portugal). *Earth and Planetary Science Letters*, **253**, 455–470, <https://doi.org/10.1016/j.epsl.2006.11.009>.

Hesselbo, S.P., Grocke, D.R., Jenkyns, H.C., Bjerrum, C.J., Farrimond, P., Morgans Bell, H.S. and Green, O.R. 2000. Massive dissociation of gas hydrate during a Jurassic oceanic anoxic event. *Nature*, **406**, 392–395, <https://doi.org/10.1038/35019044>.

Hofmann, R., Buatois, L.A., MacNaughton, R.B. and Mangano, M.G. 2015. Loss of the sedimentary mixed layer as a result of the end-Permian extinction. *Palaeogeography Palaeoclimatology Palaeoecology*, **428**, 1–11.

Howard, A.S. 1984. *Palaeoecology, sedimentology and depositional environments of the middle Lias of North Yorkshire*. PhD, University of London.

Howarth, M.K. 1992. The Ammonite family Hildoceratidae in the Lower Jurassic of Britain. *Monograph of the Palaeontographical Society*, **586**, 106pp.

IPCC. 2013. *Climate Change 2013: the Physical Science Basis*.

Jenkyns, H.C. 1988. The early Toarcian (Jurassic) anoxic event: Stratigraphic, Sedimentary, and Geochemical evidence. *American Journal of Science*, **288**, 101–151, <https://doi.org/10.2475/ajs.288.2.101>.

Jenkyns, H.C. 2010. Geochemistry of oceanic anoxic events. *Geochemistry, Geophysics, Geosystems*, **11**, 1–30, <https://doi.org/10.1029/2009GC002788>.

Jessen, G.L., Lichtschlag, A. *et al.* 2017. Hypoxia causes preservation of labile organic matter and changes seafloor microbial community composition (Black Sea). *Science Advances*, **3**, 1–14.

Jørgensen, B.B., Mortensen, P.B., Anderson, F.Ø., Rasmussen, R.A. and Jensen, A. 1995. Phosphorous cycling in a coastal marine sediment, Aarhus Bay, Denmark. *Limnology and Oceanography*, **40**, 908–917.

Karlson, K., Rosenberg, R. and Bonsdorff, E. 2002. Temporal and spatial large-scale effects of eutrophication and oxygen deficiency on benthic fauna in Scandinavian and Baltic waters - A review. *Oceanography and Marine Biology Annual Review*, **40**, 427–489, <https://doi.org/10.1201/9780203180594.ch8>.

Karlson, K., Hulth, S., Ringdahl, K. and Rosenberg, R. 2005. Experimental recolonisation of Baltic Sea reduced sediments: survival of benthic macrofauna and effects on nutrient cycling. *Marine Ecology Progress Series*, **294**, 35–49.

Kedzierski, M., Uchman, A., Sawlowicz, Z., and Briguglio, A. 2015. Fossilized bioelectric wire – the trace fossil *Trichichnus*. *Biogeosciences*, **12**, 2301–2309. <https://doi.org/10.5194/bg-12-2301-2015>, 2015, 2015.

Keeling, R.F., Körtzinger, A. and Gruber, N. 2010. Ocean Deoxygenation in a Warming World. *Annual Review of Marine Science*, **2**, 199–229.

Kemp, D.B., Coe, A.L., Cohen, A.S. and Schwark, L. 2005. Astronomical pacing of methane release in the Early Jurassic period. *Nature*, **437**, 396–399, <https://doi.org/10.1038/nature04037>.

Kemp, D.B., Coe, A.L., Cohen, A.S. and Weedon, G.P. 2011. Astronomical forcing and chronology of the early Toarcian (Early Jurassic) oceanic anoxic event in Yorkshire, UK. *Paleoceanography*, **26**, 1–17, <https://doi.org/10.1029/2011pa002122>.

Korte, C. and Hesselbo, S.P. 2011. Shallow marine carbon and oxygen isotope and elemental records indicate icehouse-greenhouse cycles during the Early Jurassic.

Paleoceanography, **26**, 1-18, <https://doi.org/10.1029/2011PA002160>.

Kristensen, E. 2000. Organic matter diagenesis at the oxic-anoxic interface in coastal marine sediments, with emphasis on the role of burrowing animals. *Hydrobiologia*, **426**, 1–24.

Kristensen, E. and Blackburn, T.H. 1987. The fate of organic carbon and nitrogen in experimental marine sediment systems: influence of bioturbation and anoxia. *Journal of Marine Research*, **45**, 231–257.

Kristensen, E., Anderson, F.Ø. and Blackburn, T.H. 1992. Effects of benthic macrofauna and temperature on degradation of macroalgal detritus: The fate of organic carbon. *Limnology and Oceanography*, **37**, 1404–1419.

Laflamme, M., Darroch, S.A.F., Tweedt, S.M., Peterson, K.J. and Erwin, D.H. 2013. The end of the Ediacara biota: Extinction, biotic replacement, or Cheshire Cat? *Gondwana Research*, **23**, 558–573, <https://doi.org/10.1016/j.gr.2012.11.004>.

Levin, L.A., Ekau, W. *et al.* 2009. Effects of natural and human-induced hypoxia on coastal benthos. *Biogeosciences*, **6**, 2063–2098, <https://doi.org/10.5194/bg-6-2063-2009>.

Little, C.T.S. 1996. The Pliensbachian-Toarcian (Lower Jurassic) extinction event. *In*: Ryder, G., Fastovsky, D. and Gartner, S. (eds) *The Cretaceous-Tertiary event and other catastrophes in Earth history*. *Geological Society of America, Special Papers*, **307**, 505–512, <https://doi.org/10.1130/0-8137-2307-8.505>.

Little, C.T.S. and Benton, M.J. 1995. Early Jurassic Mass Extinction - a Global Long-Term Event. *Geology*, **23**, 495–498, [https://doi.org/10.1130/0091-7613\(1995\)](https://doi.org/10.1130/0091-7613(1995)).

Littler, K., Hesselbo, S.P. and Jenkyns, H. 2010. A carbon-isotope perturbation at the Pliensbachian-Toarcian boundary: evidence from the Lias Group, NE England. *Geological Magazine*, **147**, 181–192, <https://doi.org/10.1017/S0016756809990458>.

Lohrer, A.M., Thrush, S. and Gibbs, M.M. 2004. Bioturbators enhance ecosystem function through complex biogeochemical interactions. *Nature*, **431**, 1092–1095.

MacEahern, J.A., Bann, K.L., Gingras, M.K., Zonneveld, J.-P., Dahstgard, S.E. and Pemberton, G.S. 2012. Chapter 4: The Ichnofacies Paradigm. *In*: Knaust, D. and Bromley, R.G. (eds) *Developments in Sedimentology*. Elsevier, The Netherlands, 103–138.

Martin, K.D. 2004. A re-evaluation of the relationship between trace fossils and dysoxia. *Geological Society London, Special Publications*, **228**, 141–156, <https://doi.org/10.1144/GSL.SP.2004.228.01.08>.

Martindale, R. and Aberhan, M. 2017. Response of macrobenthic communities to the Toarcian Oceanic Anoxic Event in northeastern Panthalassa (Ya Ha Tinda, Alberta, Canada). *Palaeogeography, Palaeoclimatology, Palaeoecology*, **478**, 103–120.

Maxwell, E.E. and Vincent, P. 2016. Effects of the early Toarcian Oceanic Anoxic Event on ichthyosaur body size and faunal composition in the Southwest German Basin. *Paleobiology*, **42**, 117–126, <https://doi.org/10.1017/pab.2015.34>.

McIlroy, D. 2004. Some ichnological concepts, methodologies, applications and frontiers. *Geological Society London, Special Publications*, **228**, 3–27, [doi:10.1144/GSL.SP.2004.228.01.02](https://doi.org/10.1144/GSL.SP.2004.228.01.02).

Mermillod-Blondin, F. 2011. The functional significance of bioturbation and biodeposition on biogeochemical processes at the water–sediment interface in freshwater and marine ecosystems. *Journal of the North American Benthological Society*, **30**, 770–778.

Meysman, F.J.R., Middelburg, J.J. and Heip, C.H.R. 2006. Bioturbation: a fresh look at Darwin's last idea. *Trends in Ecology and Evolution*, **21**, 688–694.

Miguez-Salas, O., Rodríguez-Tovar, F.J. and Duarte, L.V. 2017. Selective incidence of the Toarcian oceanic anoxic event on macroinvertebrate marine communities: a case from the Lusitanian Basin, Portugal. *Lethaia*, **50**, 548–560.

Minter, N.J., Buatois, L.A., Mangano, M.G., Davies, N.S., Gibling, M.R. and Labandeira, C. 2016. Chapter 6: The Establishment of Continental Ecosystems. In: Mangano, M.G. and Buatois, L.A. (eds) *Evolutionary Events. Topics in Geobiology 39*, Springer Science and Business Media, Dordrecht.

Molina, J.M., Reolid, M. and Mattioli, E. 2018. Thin-shelled bivalve buildup of the lower Bajocian, South Iberian paleomargin: development of opportunists after oceanic perturbations. *Facies*, **64**, 19.

Monaco, P., Nocchi, M., Ortega-Huertas, M., Palomo, I., Martinez, F. and Chiavini, G. 1994. Depositional trends in the Valdorbia section (Central Italy) during the Early Jurassic, as revealed by micropaleontology, sedimentology and geochemistry. *Eclogae Geologicae Helvetiae*, **87**, 157–223.

Morris, K.A. 1979. A classification of Jurassic marine shale sequences: An example from the Toarcian (Lower Jurassic) of Great Britain. *Palaeogeography Palaeoclimatology Palaeoecology*, **26**, 117–126.

Müller, T. Karancz, S., Mattioli, E., Milovský, R., Pálffy, J., Schlögi, J., Segit, T., Šimo, V., Tomašových, A. 2020. Assessing anoxia, recovery and carbonate production setback in a hemipelagic Tethyan basin during the Toarcian Oceanic Anoxic Event (Western Carpathians). *Global Planetary Change*, **195**, 103366.

Nikitenko, B., Reolid, M. and Glinskikh, L. 2008. Ecostratigraphy of benthic foraminifera for interpreting Arctic record of Early Toarcian biotic crisis (Northern Siberia, Russia). *Palaeogeography Palaeoclimatology Palaeoecology*, **376**, 200–212.

Norkko, J., Gammal, J., Hewitt, J.E., Josefson, A.B., Carstensen, J. and Norkko, A. 2015. Seafloor Ecosystem Function Relationships: In Situ Patterns of Change Across Gradients of Increasing Hypoxic Stress. *Ecosystems*, 1424–1439.

Norkko, A. and Bonsdorff, E. 1996. Altered benthic prey-availability due to episodic oxygen deficiency caused by drifting algal mats. *Marine Ecology*, **17**, 355–372.

Olafsson, E. 2003. Do macrofauna structure meiofauna assemblages in marine soft-bottoms? *Vie Milieu*, **53**, 249–265.

Palliani, R.B. and Riding, J.B. 1999. Relationships between the Early Toarcian anoxic event and organic-walled phytoplankton in central Italy. *Marine Micropaleontology*, **37**, 101–116.

Palliani, R.B., Mattioli, E. and Riding, J.B. 2002. The response of marine phytoplankton and sedimentary organic matter to the early Toarcian (Lower Jurassic) oceanic anoxic event in northern England. *Marine Micropaleontology*, **46**, 223–245.

Pearce, C.R., Cohen, A.S., Coe, A.L. and Burton, K.W. 2008. Molybdenum isotope evidence for global ocean anoxia coupled with perturbations to the carbon cycle during the early Jurassic. *Geology*, **36**, 231–234, doi:10.1130/G24446A.1.

Pearson, T.H. and Rosenberg, R. 1978. Macrobenthic succession in relation to organic enrichment and pollution of the marine environment. *Oceanography and Marine Biology Annual Review*, **16**, 229–311.

Pemberton, G., MacEachern, J. A., Gingras, M. K., Saunders, T. D. A. 2008 Biogenic chaos: Cryptobioturbation and the work of sedimentologically friendly organisms. *Palaeogeography, Palaeoclimatology, Palaeoecology*, **270**, 273–279.

Piazza, V., Duarte, L.V., Renaudie, J. and Aberhan, M. 2019. Reductions in body size of benthic macroinvertebrates as a precursor of the early Toarcian (Early Jurassic) extinction event in the Lusitanian Basin, Portugal. *Paleobiology*, **45**, 296–316.

Piazza, V., Ullman, C.V. and Aberhan, M. 2020. Temperature-related body size change of marine benthic macroinvertebrates across the Early Toarcian Anoxic Event. *Scientific Reports*, **10**, 4675.

Powell, J.H. 2010. Jurassic sedimentation in the Cleveland Basin: a review. *Proceedings of the Yorkshire Geological Society*, **58**, 21–72.

Rasmussen, A.D., Banta, G.T. and Andersen, O. 1998. Effects of bioturbation by the lugworm *Arenicola marina* on cadmium uptake and distribution in sandy sediments. *Marine Ecology Progress Series*, **164**, 179–188.

Reolid, M., Rivas, P. and Rodríguez-Tovar, F.J. 2015. Toarcian Ammonitico Rosso facies from the South Iberian paleomargin (Betic Cordillera, southern Spain): paleoenvironmental reconstruction. *Facies*, **61**, 22.

Reolid, M., Sebane, A., Rodríguez-Tovar, F.J. and Marok, A. 2012. Foraminiferal morphogroups as a tool to approach the Toarcian Anoxic Event in the Western Saharan Atlas (Algeria). *Palaeogeography, Palaeoclimatology, Palaeoecology*, **323–325**, 87–99, doi:10.1016/j.palaeo.2012.01.034.

Reolid, M., Emmanuela, M., Nieto, L.M. and Rodríguez-Tovar, F.J. 2014. The Early Toarcian Oceanic Anoxic Event in the External Subbetic (South Iberian palaeomargin Westernmost Tethys): Geochemistry, nannofossils and ichnology. *Palaeogeography, Palaeoclimatology, Palaeoecology*, **411**, 79–94, doi:10.1016/j.palaeo.2014.06.023.

Reolid, M., Molina, J.M., Nieto, L.M. and Rodríguez-Tovar, F.J. 2018. *The Toarcian Oceanic Anoxic Event in the South Iberian Palaeomargin*. Springer Cham, Cham, Switzerland.

Reolid, M., Copestake, P., Johnson, B. 2019. Foraminiferal assemblages, extinctions and appearances associated with the Early Toarcian Oceanic Anoxic Event in the Llanbedr (Mochras Farm) Borehole, Cardigan Bay Basin, United Kingdom. *Palaeogeography, Palaeoclimatology, Palaeoecology*, **532**, 109277. <https://doi.org/10.1016/j.palaeo.2019.109277>

Reolid, M., Mattioli, E., Duarte, L.V. and Ruebsam, W. 2021a. The Toarcian Oceanic Anoxic Event: where do we stand? *Geological Society of London Special Publications*, **514**, 185–211.

Reolid, M., Jesús Reolid, M.S., Ruebsam, W. Taher, I.B., Mattioli, E., Saidi, M., and Schwark, L. 2021b. The onset of the Early Toarcian flooding of the Pliensbachian carbonate platform of central Tunisia (north–south axis) as inferred from trace fossils and geochemistry. *Geological Society of London Special Publications*, **514**, 213–238.

Reolid, M., Ainsworth, N. A. 2022. Changes in benthic microfossil assemblages before, during and after the early Toarcian biotic crisis in the Portland-Wight Basin (Kerr McGee 97/12-1 well, offshore southern England). *Palaeogeography, Palaeoclimatology, Palaeoecology*, **599**, 11044. <https://doi.org/10.1016/j.palaeo.2022.111044>

Riedel, B., Pados, T. *et al.* 2014. Effects of hypoxia and anoxia on invertebrate behaviour: ecological perspectives from species to community level. *Biogeosciences*, **11**, 1491-1518.

Riegraf, W. 1982. The Bituminous Lower Toarcian at the Truc de Balduc near Mende (Departement de la Lozere, S-France). *In*: Einsele, G. and Seilacher, A. (eds) *Cyclic and event stratification*. Springer, Berlin, 506–511.

Rita, P., Reolid, M. and Duarte, L.V. 2016. Benthic foraminiferal assemblages record major environmental perturbations during the Late Pliensbachian–Early Toarcian interval in the Peniche GSSP, Portugal. *Palaeogeography, Palaeoclimatology, Palaeoecology*, **454**, 267–281.

Rita, P., De Baets, K. and Schlott, M. 2018. Rostrum size differences between belemnite battlefields. *Fossil Record*, **21**, 171–182.

Rita, P., Natscher, P., Duarte, L.V., Weis, R. and De Baets, K. 2019. Mechanisms and drivers of belemnite body-size dynamics across the Pliensbachian–Toarcian crisis. *Royal Society Open Science*, **6**, 190494.

Rodríguez-Tovar, F.J. 2021. Ichnology of the Toarcian Oceanic Anoxic Event: An underestimated tool to assess palaeoenvironmental interpretations. *Earth-Science Reviews*, **216**, 103579.

Rodríguez-Tovar, F.J. and Uchman, A. 2010. Ichnofabric evidence for the lack of bottom anoxia during the Lower Toarcian oceanic anoxic event in the Fuente de la Vidriera section, Betic Cordillera, Spain. *Palaios*, **25**, 576–587.

Röhl, H.-J. and Schmid-Röhl, A. 2005. Lower Toarcian (Upper Liassic) black shales of the central European epicontinental basin: A sequence stratigraphic case study from the SW German Posidonia Shale. *SEPM, Special Publication*, **82**, 165–189.

Röhl, H.-J., Schmid-Röhl, A., Oschmann, W., Frimmel, A. and Schwark, L. 2001. The Posidonia Shale (lower Toarcian) of SW Germany an oxygen-depleted ecosystem controlled by sea level and palaeoclimate. *Palaeogeography, Palaeoclimatology, Palaeoecology*, **165**, 27–52, [https://doi.org/10.1016/S0031-0182\(00\)00152-8](https://doi.org/10.1016/S0031-0182(00)00152-8).

Ros-Franch, S., Echevarría, J. *et al.* 2019. Population response during an Oceanic Anoxic Event: The case of Posidonotis (Bivalvia) from the Lower Jurassic of the Neuquén Basin, Argentina. *Palaeogeography, Palaeoclimatology, Palaeoecology*, **525**, 57–67.

Rosenberg, R. 1977. Benthic macrofaunal dynamics, production and dispersion in an oxygen-deficient estuary of west Sweden. *Journal of Experimental Marine Biology and Ecology*, **26**, 107–133.

Rosenberg, R. and Loo, L.O. 1988. Marine eutrophication induced oxygen deficiency: effects on soft bottom fauna, Western Sweden. *Ophelia*, **29**, 213–225.

Ruban, D.A. 2004. Diversity dynamics of Early-Middle Jurassic brachiopods of Caucasus, and the Pliensbachian-Toarcian mass extinction. *Acta Palaeontologica Polonica*, **49**, 275–282.

Ruebsam, W., Reolid, M., Marok, A. and Schwark, L. 2020a. Drivers of benthic extinction during the early Toarcian (Early Jurassic) at the northern Gondwana paleomargin: Implications for paleoceanographic conditions. *Earth Science Reviews*, **203**, 103117.

Ruebsam, W., Reolid, M., Sabatino, N., Masetti, D. and Schwark, L. 2020b. Molecular paleothermometry of the early Toarcian climate perturbation. *Global Planetary Change*, **195**, 103351.

Saalen, G., Doyle, P. and Talbot, M.R. 1996. Stable-isotope analyses of belemnite rostra from the Whitby mudstone Formation, England: Surface water conditions during deposition of a marine black shale. *Palaios*, **11**, 97–117.

Savrda, C.E. 2007. Chapter 6: Taphonomy of trace fossils. *In*: Miller, W.D. (ed.) *Trace fossils: Concepts, Problems, Prospects*. Elsevier, The Netherlands, 92–109.

Savrda, C.E. and Bottjer, D.J. 1986. Trace fossil model for reconstruction of palaeo-oxygenation in bottom-waters. *Geology*, **14**, 3–6.

Savrda, C.E. and Bottjer, D.J. 1987. The exaerobic zone, a new oxygen deficient marine biofacies. *Nature*, **327**, 54–56.

Savrda, C.E. and Bottjer, D.J. 1989. Anatomy and implications of bioturbated beds in “Black Shale” sequences: Examples from the Jurassic Posidonienschiefer (Southern Germany). *Palaios*, **4**, 330–342.

Scheiber, J. 2002. The role of an organic slime matrix in the formation of pyritized burrow trails and pyrite concretions. *Palaios*, **17**, 104–109.

Schlirf, M. 2011. A new classification concept for U-shaped spreite trace fossils. . *Neues Jahrbuch für Geologie und Paläontologie, Abhandlungen*, **260**, 33–54.

Schwark, L. and Frimmel, A. 2004. Chemostratigraphy of the Posidonia Black Shale, SW-Germany II. Assessment of extent and persistence of photic-zone anoxia using aryl isoprenoid distribution. *Chemical Geology*, **206**, 231–248.

Seilacher, A. 2007. *Trace Fossil Analysis*. Springer-Verlag, Berlin.

Seilacher, A., Buatois, L.A. and Mangano, M.G. 2005. Trace fossils in the Ediacaran–Cambrian transition: behavioral diversification, ecological turnover and environmental shift. *Palaeogeography, Palaeoclimatology, Palaeoecology*, **227**, 323–356.

Šimo, V. and Reolid, M. 2021. Palaeogeographical homogeneity of trace-fossil assemblages in Lower Jurassic spotted marls and limestones: comparison of the Western Carpathians and the Betic Cordillera. *Geological Society London, Special Publications*, **514**, 185–211. <https://doi.org/10.1144/SP514-2020-110>

Smith, C.R., Levin, L.A., Hoover, D.J., McMurry, G. and Gage, J.D. 2000. Variations in bioturbation across the oxygen minimum zone in the northwest Arabian Sea. *Deep-Sea Research II* **47**, 227–257.

Smith, F.A. and Lyons, K.S. 2013. *Animal body size: Linking patterns and process across space, time and taxonomic group*. University of Chicago Press, Chicago, USA.

Snelgrove, P.V. 1997. The importance of marine sediment biodiversity in ecosystem processes. *Ambio*, **26**, 578–583.

Snelgrove, P.V. 1999. Getting to the Bottom of Marine Biodivers: Sedimentary habitats. *BioScience*, **49**, 129–138.

Snelgrove, P.V., Thrush, S.F., Wall, D.H. and Norkko, A. 2014. Real world biodiversity-ecosystem functioning: a seafloor perspective. *Trends in Ecology & Evolution*, **29**, 398–405.

Snelgrove, P.V., Soetaert, K., Soetaert, K., Solan, M., Thrush, S., Wei, C.-L., Danovaro, R., Fulweiler, R. W., Kitazato, H., Ingole, B., Norkko, A., Parkes, R. J., Volkenborn, V. 2018. Global Carbon Cycling on a Heterogeneous Seafloor. *Trends in Ecology & Evolution*, **33**, 96–105.

Solan, M. and Wigham, B.D. 2005. Biogenic particle reworking and bacterial-invertebrate interactions in marine sediments. In: Kristensen, E., Haese, R.R. and Kostka, J.E. (eds) *Macro- and Micro-organisms in Marine Sediments. Coastal and Estuarine Studies*, 60, American Geophysical Union, Washington, DC, 105–124.

Solan, M., Bennett, E.M., Mumby, P.J., Leyland, J. and Godbold, J.A. 2020. Benthic-based contributions to climate change mitigation and adaptation. *Philosophical Transactions - Royal Society of London, B*, **375**, 20190107, <https://doi.org/10.1098/rstb.2019.0107>.

Solan, M., Cardinale, B.J., Downing, A.L., Engelhardt, K.A.M., Ruesink, J.L. and Srivastava, D.S. 2004. Extinction and ecosystem function in the marine benthos. *Science*, **306**, 1177–1180.

Solan, M., Ward, E.R. *et al.* 2019. Worldwide measurements of bioturbation intensity, ventilation rate, and the mixing depth of marine sediments. *Scientific Data*, **6**, 58. doi:10.1038/s41597-019-0069-7

Sperling, E. 2013. Tackling the 99%: Can We Begin to Understand the Paleoecology of the Small and Soft-Bodied Animal Majority? *The Paleontological Society Papers*, **19**, 77–86. doi:10.1017/S1089332600002692

Stachowitsch, M. 1991. Anoxia in the Northern Adriatic Sea: Rapid death, slow recovery. *Geological Society London, Special Publications*, **58**, 119–1291.

Stramma, L., Schmidtko, S., Levin, L.A. and Johnson, G.C. 2010. Ocean oxygen minima expansions and their biological impacts. *Deep-Sea Research Part I-Oceanographic Research Papers*, **57**, 587–595. doi: 10.1016/j.dsr.2010.01.005.

Suan, G., Pittet, B., Bour, I., Mattioli, E., Duarte, L.V. and Mailliot, S. 2008. Duration of the Early Toarcian carbon isotope excursion deduced from spectral analysis: Consequence for its possible causes. *Earth and Planetary Science Letters*, **267**, 666–679.

Suan, G., Nikitenko, B.L. *et al.* 2011. Polar record of Early Jurassic massive carbon injection. *Earth and Planetary Science Letters*, **312**, 102–113.

Teal, L.R., Bulling, M.T., Parker, E.R. and Solan, M. 2008. Global patterns of bioturbation intensity and mixed depth of marine soft sediments. *Aquatic Biology*, **2**, 207–218.

Them, T.R., Gill, B.C., Selby, D., Gröcke, D.R., Friedman, R.M. and Owens, J.D. 2018. Evidence for rapid weathering response to climatic warming during the Toarcian Oceanic Anoxic Event. *Scientific Reports*, 5003.

Them, T.R., Gill, B.C. *et al.* 2019. Thallium isotopes reveal protracted anoxia during the Toarcian (Early Jurassic) associated with volcanism, carbon burial, and mass extinction. *Proceedings of the National Academy of Science*, **115**, 6596–6601.

Tomašových, A., Gallmetzer, I., Haselmair, A., Kaufman, D. S., Krald, M., Cassin, D., Zonta, R., Zuschin, M. 2018. Tracing the effects of eutrophication on molluscan communities in sediment cores: outbreaks of an opportunistic species coincide with reduced bioturbation and high frequency of hypoxia in the Adriatic Sea. *Paleobiology*, **44**, 575–602.

Tomašových, A., Albano, P. G., Fuksi, T., Gallmetzer, I., Haselmair, A., Kowalewski, M., Nawrot, R., Nerlovic, V., Scarponi, D., Zuschin, M. 2020. Ecological regime shift preserved in the Anthropocene stratigraphic record. *Proceedings of the Royal Society B*, **287**, 20200695. doi:10.1098/rspb.2020.0695.

Tomašových, A., Berensmeier, M., Gallmetzer, I., Haselmair, A., Zuschin, M. 2021. Pyrite-lined shells as indicators of inefficient bioirrigation in the Holocene–Anthropocene stratigraphic record. *Biogeosciences*, **18**, 5929–5965.

Thrush, S.F., Hewitt, J.E., Lohrer, A.M. and Chiaroni, L.D. 2013. When small changes matter: the role of cross-scale interactions between habitat and ecological connectivity in recovery. *Ecological Applications*, **23**, 226–238.

Trabucho-Alexandre, J., Dirx, R., Veld, H., Klaver, G. and de Boer, P.L. 2012. Toarcian Black Shales In the Dutch Central Graben: Record of Energetic, Variable Depositional Conditions During An Oceanic Anoxic Event. *Journal of Sedimentary Research* **82**, 104–120.

Trabucho-Alexandre, J., Grocke, D.R., Atar, E., Herringshaw, L.G. and Jarvis, I. 2022. A New Subsurface Record of the Pliensbachian-Toarcian, Lower Jurassic, of Yorkshire. *Proceedings of the Yorkshire Geological Society*, 64 (2), 1–12, doi:10.1144/pygs2022-007

Twitchett, R.J. and Barras, C.G. 2004. Trace fossils in the aftermath of mass extinction events. *Geological Society London, Special Publications*, **228**, 397–418, doi:10.1144/GSL.SP.2004.228.01.18.

Uchman, A. 1995. Taxonomy and palaeoecology of flysch trace fossils: the Marnoso-arenacea Formation and associated facies (Miocene, Northern Apennines, Italy), *Beringeria*, **15**, 3–115, 1995.

Uchman, A. 1999. Ichnology of the Rhenodanubian Flysch (Lower Cretaceous–Eocene) in Austria and Germany, *Beringeria*, **25**, 65–171.

van Acken, D., Tütken, T., Daly, J.S., Schmid-Röhl, A. and Orr, P.J. 2019. Rhenium-osmium geochronology of the Toarcian Posidonia Shale, SW Germany. *Palaeogeography, Palaeoclimatology, Palaeoecology*, **534**, 109294.

van Breugel, Y., Baas, M., Schouten, S., Mattioli, E. and Damste, J.S.S. 2006. Isorenieratane record in black shales from the Paris Basin, France: Constraints on recycling of respired CO₂ as a mechanism for negative carbon isotope shifts during the Toarcian oceanic anoxic event. *Paleoceanography*, **21**, 1–8.

Van de Schootbrugge, B., Bachan, A., Suan, G., Richoz, S. and Payne, J.L. 2013. Microbes, mud and methane: Cause and consequence of recurrent early Jurassic anoxia following the end-Triassic mass extinction. *Palaeontology*, **56**, 685–709, doi:10.1111/pala.12034.

Vasseur, R., Lathuilière, B., Lazar, I., Martindale, R. C. Bodin, S., Durlet, C. 2021. Major coral extinctions during the early Toarcian global warming event. *Global Planetary Change*, **207**, 103647.

Volkenborn, N., Hedtkamp, S.I.C., Van Beusekom, J.E.E. and Reise, K. 2007. Effects of bioturbation and bioirrigation by lugworms (*Arenicola marina*) on physical and chemical sediment properties and implications for intertidal habitat succession. *Estuarine, Coastal and Shelf Science* **74**, 331–343.

Vörös, A. 2002. Victims of the Early Toarcian anoxic event: the radiation and extinction of Jurassic Koninckinidae (Brachiopoda). *Lethaia*, **35**, 345–357.

Warwick, R.M. and Clarke, K.R. 1984. Species size distributions in marine benthic communities. *Oecologia*, **61**, 32–41.

Wiest, L.A., Buyenvich, I.V., Grandstaff, D.E., Terry Jr., D.O. and Maza, Z.A. 2015. Trace fossil evidence suggests widespread dwarfism in response to the end-Cretaceous mass

extinction: Braggs, Alabama and Brazos River, Texas. *Palaeogeography, Palaeoclimatology, Palaeoecology*, **417**, 105–111.

Wignall, P.B., Newton, R.J. and Little, C.T.S. 2005. The timing of paleoenvironmental change and cause -and-effect relationships during the Early Jurassic mass extinction in Europe. *American Journal of Science*, **305**, 1014–1032.

Xu, W., Ruhl, M. *et al.* 2018. Evolution of the Toarcian (Early Jurassic) carbon-cycle and global climatic controls on local sedimentary processes (Cardigan Bay Basin, UK). *Earth and Planetary Science Letters*, **484**, 396–411.

Zakharov, V.A., Shurygin, B.N., Il'ina, V.I. and Nikitenko, B.L. 2006. Pliensbachian-Toarcian biotic turnover in north Siberia and the Arctic region. *Stratigraphy and Geological Correlation*, **14**, 399–417.

ACCEPTED MANUSCRIPT

Figure Captions

Fig. 1. Stratigraphical log of the late Pliensbachian–early Toarcian of Yorkshire, UK with ammonite biostratigraphy and lithology (Howarth 1992; Kemp *et al.* 2011). Lithology for the Cleveland Ironstone Formation is from Howarth (1955) except beds 34–42 which are from Caswell and Coe (2014). The Whitby Mudstone Formation lithology is from Kemp *et al.* (2005) up to bed 52, beds 53–72 is from Howarth (1962). Bed numbers and ammonite biostratigraphy are from Howarth (1992). Geochemical proxies for water temperature ($\delta^{18}\text{O}_{\text{beI}}$), palaeoredox (sedimentary Re/Mo), Total Organic Carbon content (% by weight) and carbon isotopes ($\delta^{13}\text{C}_{\text{Org}}$) are from Saelen *et al.* (1996); Bailey *et al.* (2003); Cohen *et al.* (2004); Harding (2004); Kemp *et al.* (2005); Pearce *et al.* (2008); Littler *et al.* (2010); Kemp *et al.* (2011); Korte and Hesselbo (2011). Extinction horizons (ii) and (iii) are from Caswell *et al.* (2009). Geochemical palaeoredox interpretations are from Pearce *et al.* (2008) and records: the progression from oxic to regionally anoxic conditions before the OAE (*paltum-tenuicostatum* Subzone); globally anoxic conditions during the OAE (upper *semicelatum-exaratum* Subzone); regional anoxia–hypoxia (*falciferum* to lower half of the *commune* Subzone). The period after those proposed by Pearce *et al.* (2008) may represent more oxygenated conditions (based on sedimentology and geochemistry; Cohen *et al.* 2004, Kemp *et al.* 2011). The *H. falciferum* Zone is equivalent to the *Harpoceras serpentinum* Zone in the Tethyan sections. Ammonite zone and subzone abbreviations: A. gib. = *Amaltheus gibbosus*, A. mar. = *Amaltheus margaritatus*, C. exaratum = *Cleviceras exaratum*, C. crass. = *Catacoeloceras crassum*, D. c. = *Dactylioceras clevelandicum*, *Dactylioceras commune*, D. semi. = *Dactyliocerasemicelatum*, D. t. = *Dactylioceras tenuicostatum*, H. falciferum = *Harpoceras falciferum*, P. fibulat. = *Peronoceras fibulatum*, Pl. apy. = *Pleuroceras apyrenum*, Pl. haw. = *Pleuroceras hawskerense*, Pl. spinatum = *Pleuroceras spinatum*, P. paltum = *Protogrammoceras paltum*.

Fig. 2. Stratigraphic logs from the six NE Yorkshire coastal sections and core N1 (Fig. S1) with trace fossil ranges for each. Lithology for the Cleveland Ironstone Formation at Hawsker Bottoms (HB), Kettlewell (KN), and Staithes (ST) for beds 22–33 are from Howarth (1955); and, beds 34–42 at HB are from Caswell and Coe (2014). The Whitby Mudstone Formation lithology for HB, Port Mulgrave (PM) and Saltwick Bay (SB; beds 42–52) are from Kemp *et al.* (2005). The lithology for beds 53–72 at SB and the complete section at Ravenscar (RA) are from Howarth (1962). Bed numbers and ammonite biostratigraphy from the coastal sections are from Howarth (1992). Biostratigraphic correlations between ST, KN, HB and PM are after Howarth (1955, 1973, 1962, 1992); and the correlation between SB and RA to the SE of Peak

Fault are after Howarth (1962, 1992). Lithology for core N1 from 126 to 200 m is from Trabucho-Alexandre *et al.* (2022), and the remainder is from this study, correlation between the core and the coastal sections (indicated by broken lines) uses geochemistry and is also from Trabucho-Alexandre *et al.* (2022). “?” indicates a degree of uncertainty on correlations. For descriptions of the various trace fossil morphologies see Tables 1-2, and supplementary Tables S1–S2.

Fig. 3. Annotated photographs of selected intervals from the coastal exposures. Trace fossils on bedding surfaces in: (A) bed 21 at Kettleness, (B) bed 19 nodules at Kettleness, (C) bed 27 and (D) bed 26–27 at Hawsker Bottoms. (E) Cross-section through bed 26–27 and (F) changing ichnofabric index visible in cross section through bed 25–27 at Kettleness. Trace fossils in (G)–(H) the top of bed 41, and (I) in cross-section at Hawsker Bottoms. Ichnofabric index after Droser and Bottjer (1986); where ichnofabric: 1 = zero evidence for bioturbation; 2 = <10% bioturbated; 3 = 10–40% bioturbated; 4 = 40–60% bioturbated; 5 = >60% bioturbated. Abbreviations: *Ch* = *Chondrites*, *Di* = *Diplocraterion*, *Rz* = *Rhizocorallium*, *Th* = *Thalassinoides*, *sp* = spreiten. Scale bar = 2 cm.

Fig. 4. Annotated photographs of selected intervals from the coastal exposures between Saltwick Bay and Whitby West Cliff (A–G), Port Mulgrave (H), Kettleness and Hawsker Bottoms (I–K). (A) Top of bed 72 (mudrock with small siderite nodules visible in the foreground and one large nodule below the Dogger Fm). A disconformity lies at the contact between the top of bed 72 and the Aalenian Dogger Fm. (B) Underside of a loose block of the Dogger Fm. in Long Bight, and (C)–(E) pyritised trace fossils in bed 53 in Rail Hole Bight. Trace fossils in bedding planes of (F) bed 52 between Rail Hole Bight and Jump Down Bight; and, (G) the top of bed 48 at Jump Down Bight. (H) Bedding planes in bed 31 at Blea Wyke, Port Mulgrave. In bedding surfaces of (I)–(J) bed 30 at Kettleness and Hawsker Bottoms, respectively, and (K) the top of bed 28 at Kettleness. Abbreviations: *Ch* = *Chondrites*, ?*Op* = ?*Ophiomorpha*, *Op* = *Ophiomorpha*, *Pa* = *Palaeophycus*, *Rz* = *Rhizocorallium*, *Th* = *Thalassinoides*, ?*Tr* = ?*Trichichnus* sp. A, *sp* = spreiten, *sc* = scratches, *t* = tubes, *be* = belemnite. Scale bar for A–B = 8 cm, and C–J = 2 cm.

Fig. 5. Composite log of the Yorkshire coast section and core N1 showing the number of ichnotaxa ($n=700$), ichnofabric index ($n = 677$), maximum burrow diameter ($n = 664$), burrow orientation in relation to bedding, and the presence/absence of pyritised burrows and sedimentary laminae. Body fossil diversity and abundance for the coastal exposures is also shown (from Caswell and Frid 2017). Ichnofabric index after Droser and Bottjer (1986); where ichnofabric: 1 = zero evidence for bioturbation; 2 = <10% bioturbated; 3 = 10–40% bioturbated; 4 = 40–60% bioturbated; 5 = >60%

bioturbated. N = number of stratigraphic sampling levels this varied somewhat, between ichnotaxa number, ichnofabric index and maximum burrow diameter, on different sampling days or secondary data sources. Lithology, lithostratigraphy, bed numbers, biostratigraphy and abbreviations as for Fig. 1. Scale of the composite log and core N1 is approximately 1:1, ties lines correlating the two logs are as for Fig. 2. Palaeoredox interpretations are as for Fig. 1, but include interpretations from trace fossil and body fossil data presented in this study; including for the preceding late Pliensbachian *spinatum* Zone, oxygenation events at subzone boundaries, and changes during the *bifrons* Zone (mid *commune* to *crassum* Subzones). Stage boundary is indicated by double horizontal line on biostratigraphic column.

Fig. 6. Composite log of the Yorkshire coast section with the abundance of each feeding mode, sediment depth, the five bioturbatory modes, and total number of bioturbatory modes present at each stratigraphic level. Surface dwelling forms are not plotted as no ichnotaxa were interpreted as being produced by epifauna. Interpretations of trace fossil behaviour are classified according to Table 2. The trace fossil behaviours are considered within the context of body fossil feeding mode and life habit (from Caswell and Frid 2017). Lithology, lithostratigraphy, bed numbers, biostratigraphy, interpretation of palaeoenvironmental changes and abbreviations as for Fig. 1; palaeoredox interpretations are as for Fig. 5. Stage boundary is indicated by double horizontal line on biostratigraphic column.

Fig. 7. Composite log of core N1 showing with the abundance of each feeding mode, sediment depth, the five bioturbatory modes, and total number of bioturbatory modes present at each stratigraphic level. Surface dwelling forms are not plotted as no ichnotaxa were interpreted as being produced by epifauna. Interpretations of trace fossil behaviour are classified according to Table 2. Lithology, lithostratigraphy, bed numbers, biostratigraphy, interpretation of palaeoenvironmental change and abbreviations as for Fig. 1; correlation between core and outcrop as for Fig. 5; palaeoredox interpretations are as for Fig. 5. Stage boundary is indicated by double horizontal line on biostratigraphic column.

Table Captions

Table 1. Scheme used to classify a range of straight/sinuuous trace fossil morphotypes that did not fit into established ichnogenera. A total of 7 morphotypes were described (Table S1).

Table 2. Biological traits and modalities used to classify Pliensbachian–Toarcian fossils in Yorkshire, UK. Traces were classified first on the basis of directly observable/measurable trace attributes (A–H) and from these behavioural traits (I, J, K, L) were interpreted. The data used and rationale for each interpretation is provided. See Tables S1 and S2 for classification of the individual ichnogenera and sources of information used.

Table 3. Median number of ichnotaxa, ichnofabric index, maximum burrow diameter and the number of bioturbatory modes present for each ammonite subzone on the coast and in the core. Raw data are plotted through time on Fig. 5. Hyphens indicate insufficient data to calculate medians. Letters in superscript (a–i) indicate no significant difference between the medians (Kruskal-Wallis tests, $p > 0.05$) in pairwise comparisons for those sharing that letter. OAE (*exaratum* subzones) is shaded in grey, but note this begins in the upper part of the *semicelatum* Subzone. “Pliens.” = Pliensbachian.

Diameter (mm)	Morphology	Orientation	Taphonomy
<3	Straight	Horizontal (h) or oblique (o)	Pyritised
3–5	Branching	Vertical (v)	Not-pyritised
5–10	Annulated		
>10			

ACCEPTED MANUSCRIPT

Table 1

Trait	Modalities	Data used and interpretation
Trace morphology and morphometrics		
(A) Max. trace diameter (mm)*	(1) ≤ 3 , (2) 3.1–5, (3) 5.01–10, (4) 10.01–20, (5) >20.01	Burrow diameters are used as a proxy for trace-maker body-size. As far as possible, only the inhabited portion of the trace is considered (e.g., <i>Rhizcorallium</i> tubes), and so depends on the interpretations of behaviour (see Table S1)
(B) Gross morphology	(1) Unbranched, (2) Intermittent branching (≤ 1 per length), (3) Regular branching (2–5 per length), (4) Highly branched (≥ 6 per length)	Determined from trace morphology. Expressed as the number branches originating from a trace length that measures 10x the trace diameter. B1 includes all unbranched forms whatever the shape (e.g., linear, meandering, u-shaped).
(C) Trace orientation	(1) Horizontal or oblique, (2) Vertical, (3) Both horizontal and vertical	Determined from trace morphology
(D) Maximum depth (mm) of vertical component*	(1) None; (2) 0–5.01; (3) 5.01–10; (4) 10.01–50; (5) >50.01	Determined from measurements of traces
(E) Burrow lining	(1) Unlined, (2) thin lining (≤ 2 mm), (3) thick lining (>2 mm), (4) thick lining with feeding pellets, (5) Not a burrow	Determined from observation
(F) Evidence for excavation	(1) Burrow without spreiten/menisci, (2) Burrow with spreiten, (3) Burrow with spreiten and faecal pellets, (4) Burrow with menisci, (5) Not a burrow	Determined from observation. Spreiten indicate active sediment movement (during excavation and/or deposit feeding), pellets within spreiten are of faecal origin, and menisci suggest active backfilling.
(G) Ornamentation	(1) Bioglyphs present (2) bioglyphs absent	Bioglyphs such as scratches demonstrate excavation, burrow maintenance or deposit feeding.
(H) Burrow complexity	(1) Single tube with ≤ 1 opening, (2) Single tube with >1 opening, (3) Branching morphology with multiple openings, (4) Branching morphology with multiple openings and chambers [§] , (5) Not a burrow	Determined from trace morphology. Complexity increases as traces occupy more dimensions, the number of entrances and exits increase, and a greater range of different burrow features, e.g. chambers, are added.
Interpreted behavioral traits (from A–H)		
(I) Feeding mode	(1) Deposit feeder/grazer, (2) Scavenger/predator, (3) suspension/filter feeder	(I1) Deposit feeding (DF) is indicated by constant searching of sediment for food. Systematic searching produces spreiten (F2) or menisci (as backfill; F4) which may contain faecal pellets (F3). Bioglyphs (G2) can indicate burrow excavation/maintenance and DF. Tubes lined with feeding pellets (E4) are also indicative of sediment ingestion. Burrows tend to be complex (H2–H4), although surface deposit feeders might use simple burrows other evidence of sediment working is also expected. Surface grazing by snails indicated by meandering grazing trails (C1, D2). (I2) SF/filter feeders occupy vertical (C2–3) burrows which are simple (H1–2), and permanent (so may be maintained (G2) and/or have a lining; E2–3). (I3) Can be hard to distinguish in the fossil record, vertical burrows (C2–C3) and open networks are often used for passive carnivory. Distinct features of DF are lacking (F2–3, F1).
(J) Minimum likely sediment depth (mm) †	(1) Surface; (2) Semi-infaunal (0–5 mm); (3) Shallow infaunal (5.01–50 mm); (4) Deep infaunal (>50.1 mm).	(J1) Horizontally oriented (C1), surface (D1) trace of any morphology (B1–B5) and size (A1–5) without distinct morphological characters (E5, F4, G2, H5) (J2) Horizontally oriented (C1), simple (H1, H5) unlined burrows (E1) or not a burrow (E5), of any size (A1–A5), and morphology (B1–B2). Produced near to sediment surface (D2). (J3) Vertical (C2–3) components between 5 and 50 mm (D3–4). Burrows, of any morphology (B1–4), size (A1–5) or complexity (H1–4). Horizontal burrows (C1) without a vertical component preserved (D1) are assumed to fall within

		J3 if burrow diameter is A2–A4. (J4) As for J3 except vertical components >50.01 mm (D5)
(K) Bioirrigation	(1) Highly improbable; (2) Improbable; (3) Probable; (4) Required.	Likelihood burrow/trace was bioirrigated based on whether it was: (K1) at the sediment surface (J1); (K2) near the sediment surface (J2); (K3) shallow (J3) and requiring short-term irrigation; (K4) a permanent subsurface dwelling (K4), with a more complex structure (H3–4) would require short-term irrigation. Creation of a chemically distinct bioirrigated environment is supported by the presence of a burrow lining (E2–4).
(L) Bioturbatory mode [‡]	(1) Epifaunal locomotion, (2) Surficial modification, (3) Biodiffusor [§] , (4) [§] Upward-conveying/ regenerators, (5) Downward-conveying, (6) Gallery biodiffusors	(L1) Horizontally oriented (C1) surface trace (J1, D1, E5, F4, G2, H5) of any morphology (B1–4), feeding mode (D1–3) and size (A1–5). (L2) Horizontally oriented, unlined burrows >3 mm, diameter, that are shallow (J2–3) unbranched or intermittently branched, not complex (H1–2) not bioirrigated (K1–2) (L3) Homogenized sediments near surface, lacks discrete trace, bioirrigation improbable. (L4) Vertical (C2–3), unbranched or branched (B1–3), simple to intermediate (C1–3), shallow to deep (J2–3), often but not exclusively deposit feeders (I1), bioirrigation possible (K2–3), (L5) Vertical (C2–3), unbranched or branched (B1–3), simple (H1–2), shallow to deep (J2–3), with faecal pellets (F3), bioirrigation possible (K2–3) (L6) Vertically and horizontally oriented (D3), branched (C2–3), complex (H3–4) probably lined (E2–4), spreiten or menisci (F2–4) and/or bioglyphs (G1) might be present, bioirrigation likely (K3–4)

*Estimates depend somewhat on interpretation of ichnogenera behaviour (See SI Table S1). [†]Burrowing depths after Bambach et al. (2007) and Minter et al. (2016); in the present-study these are inferred from interpreted behaviour and morphometrics (D); although all burrows will access the surface there will be some uncertainty because the uppermost part/surface expression of a burrow are not often preserved.

[‡]Bioturbatory modes after Solan & Wigham (2005), except for upward-conveying and regenerators which are combined because they cannot be distinguished from each other in the trace fossil record. [§]Includes *Phoebichnus* a morphology with one central chamber and c. 18 radial tubes which connect to the surface, technically the radial tubes do not “branch” but they are comprised of multiple elements, occupy multiple dimensions, and have multiple surface openings and so are considered to be complex. [¶]See also sediment homogenization metric.

Stage	Ammonite zone	Ammonite subzone	Medians			
			Ichnotaxon number	Ichnofabric index	Max. burrow diameter	No. bioturbatory modes
Coastal sections						
Toarcian	<i>bifrons</i>	<i>crassum</i>	1.00 ^{a,b,c}	2.00 ^{a,b,d}	5.00 ^c	1.00 ^{a,b}
		<i>fibulatum</i>	1.00 ^{a,b,f}	2.00 ^a	4.80 ^c	1.00 ^{a,b}
		<i>commune</i>	0.00 ^a	2.00 ^a	0.00 ^{d,e}	0.00 ^c
	<i>falciferum</i>	<i>falciferum</i>	0.00 ^e	1.00 ^g	0.00 ^f	0.00 ^e
		<i>exaratum</i>	0.00 ^e	1.00 ^g	0.00 ^f	0.00 ^e
	<i>tenuicostatum</i>	<i>semicelatum</i>	0.00 ^d	1.00 ^f	0.00 ^e	0.00 ^{c,e}
		<i>tenuicostatum</i>	0.00 ^{a,d}	1.50 ^{a,e,f}	0.00 ^{a,c,e}	0.00 ^{a,c,e}
		<i>clevelandicum</i>	0.00 ^{a,b,d}	1.00 ^{a,e,f,g}	0.00 ^{b,c,e}	0.00 ^{a,c,e}
		<i>paltum</i>	1.00 ^{a,c}	2.00 ^{a,e}	2.00 ^{b,c,d}	2.50 ^{a,d}
Pliens.	<i>spinatum</i>	<i>hawkerense</i>	2.00 ^{c,g}	3.00 ^{b,c,d}	10.00 ^{a,b}	3.00 ^b
		<i>apyrenum</i>	4.00 ^{f,g}	4.00 ^c	27.00 ^a	3.00 ^{b,d}
	<i>margaritatus</i>	<i>gibbosus</i>	3.00 ^{b,c,g}	2.00 ^{a,c}	5.00 ^{a,c}	1.50 ^{b,c,d}
		Core N1				
Toarcian	<i>bifrons</i>	<i>crassum</i>	-	-	-	-
		<i>fibulatum</i>	-	-	-	-
		<i>commune</i>	1.00 ^{a,b}	2.50 ^{a,b}	2.00 ^{a,b}	1.00 ^{a,b}
	<i>falciferum</i>	<i>falciferum</i>	0.00 ^a	1.00 ^a	0.00 ^a	0.00 ^a
		<i>exaratum</i>	0.00 ^{a,b}	1.00 ^{a,b}	0.00 ^{a,b}	0.00 ^{a,b}
	<i>tenuicostatum</i>	<i>semicelatum</i>	0.00 ^{a,b}	1.00 ^{a,b}	0.00 ^{a,b}	0.50 ^{a,b}
		<i>tenuicostatum</i>	1.00 ^{a,b}	2.00 ^{a,b}	3.00 ^{a,b}	3.00 ^{a,b}
		<i>clevelandicum</i>	1.00 ^{a,b}	2.00 ^{a,b}	3.00 ^{a,b}	1.00 ^{a,b}
Pliens.	<i>spinatum</i>	<i>paltum</i>	1.00 ^{a,b}	2.00 ^{a,b}	0.00 ^b	3.00 ^b
		<i>hawkerense</i>	2.00 ^b	4.00 ^b	10.00 ^{a,b}	2.00 ^{a,b}
	<i>margaritatus</i>	<i>apyrenum</i>	-	-	-	-
		<i>gibbosus</i>	-	-	-	-

Table 3

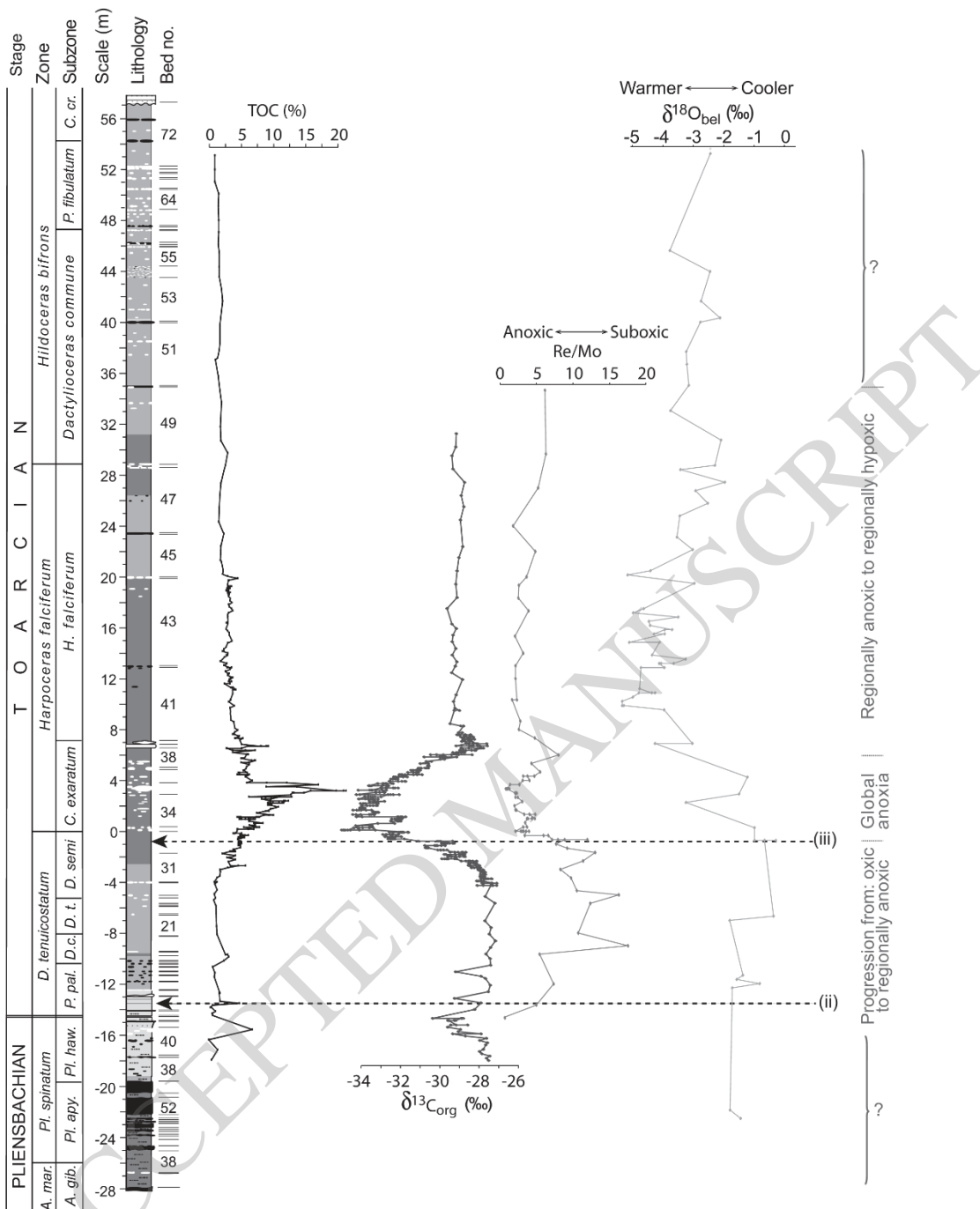


Figure 1

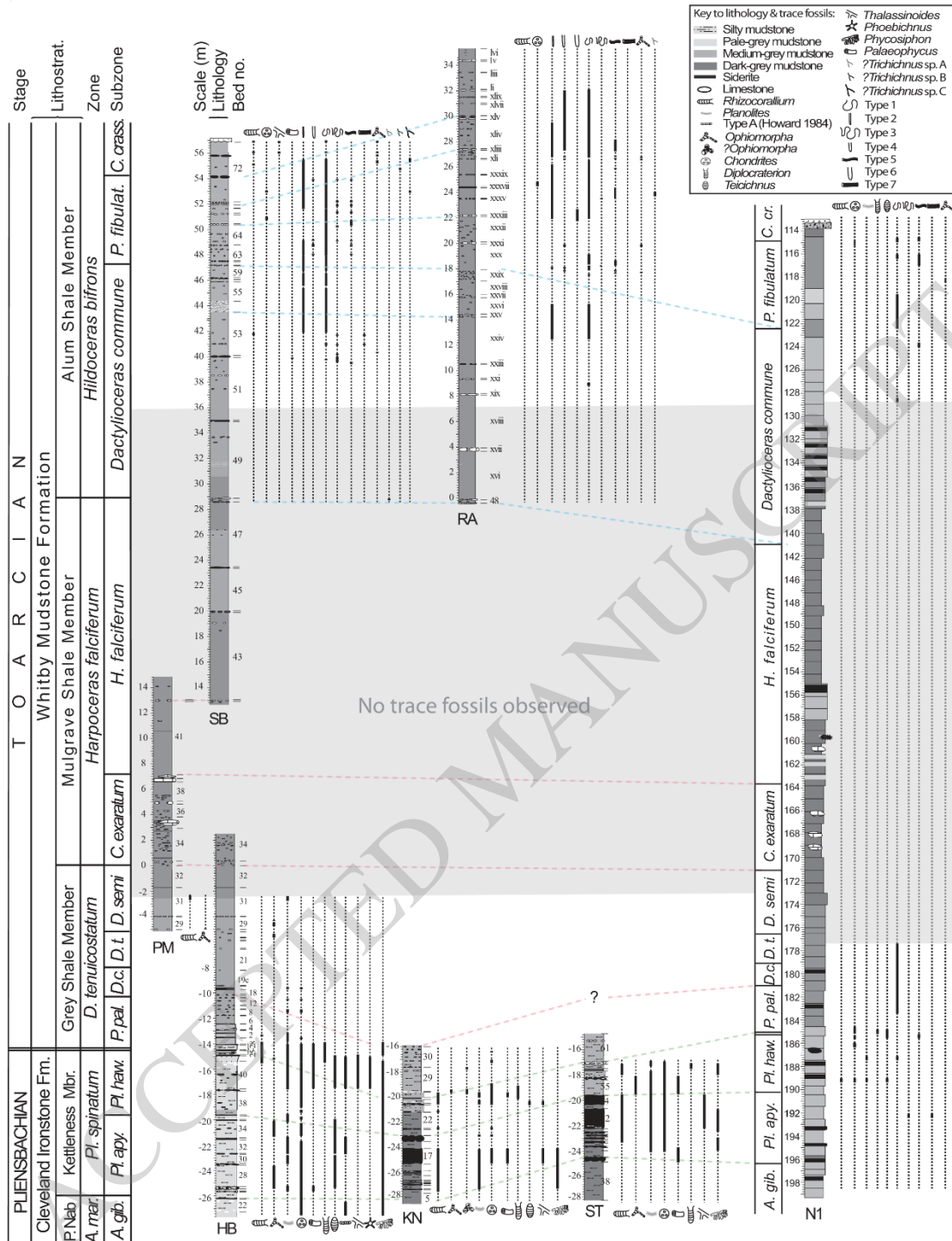


Figure 2

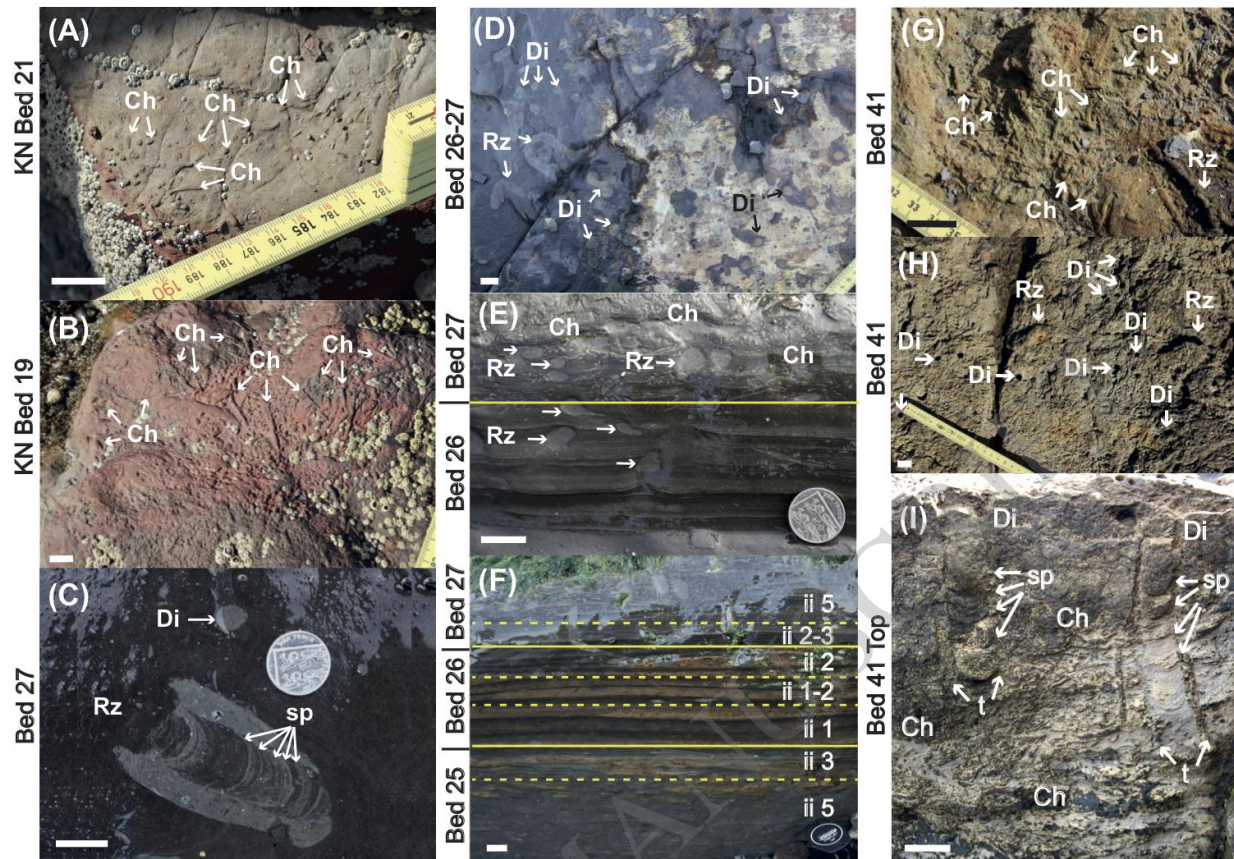


Figure 3

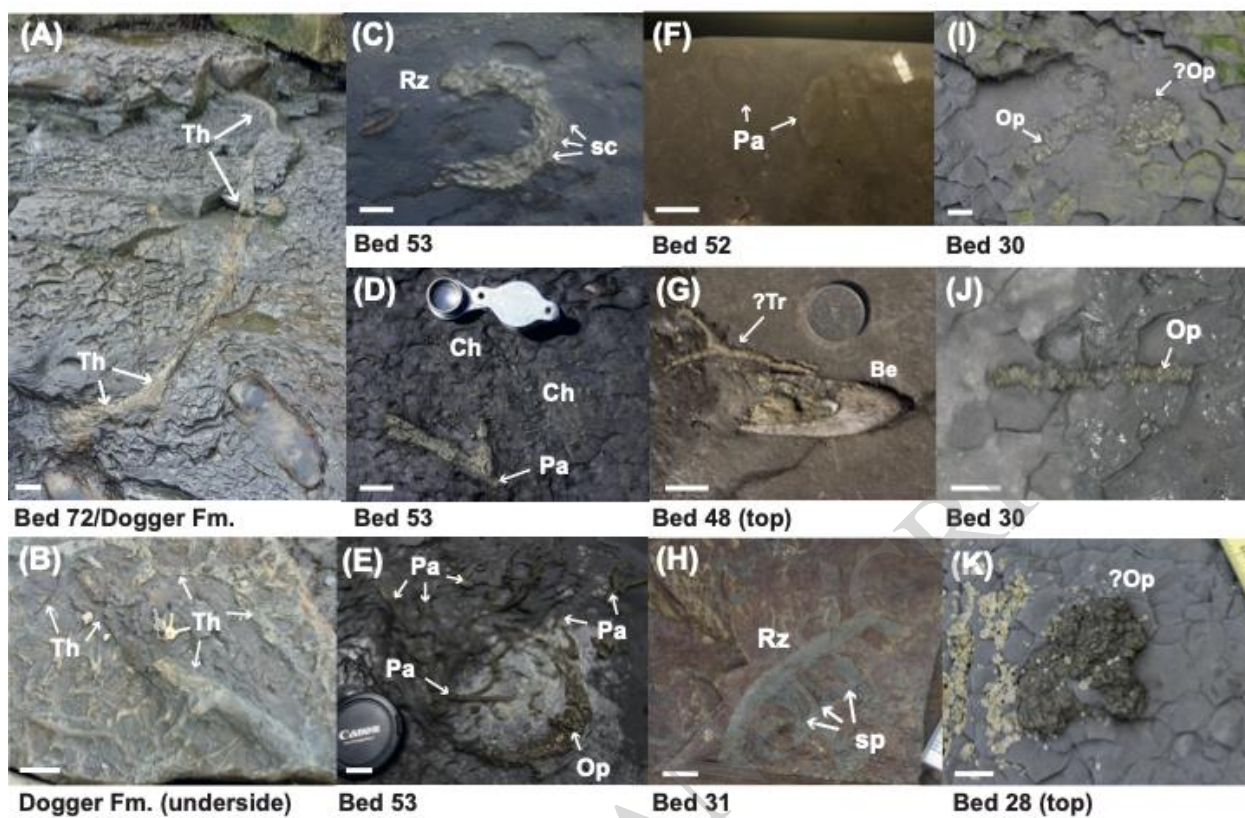


Figure 4

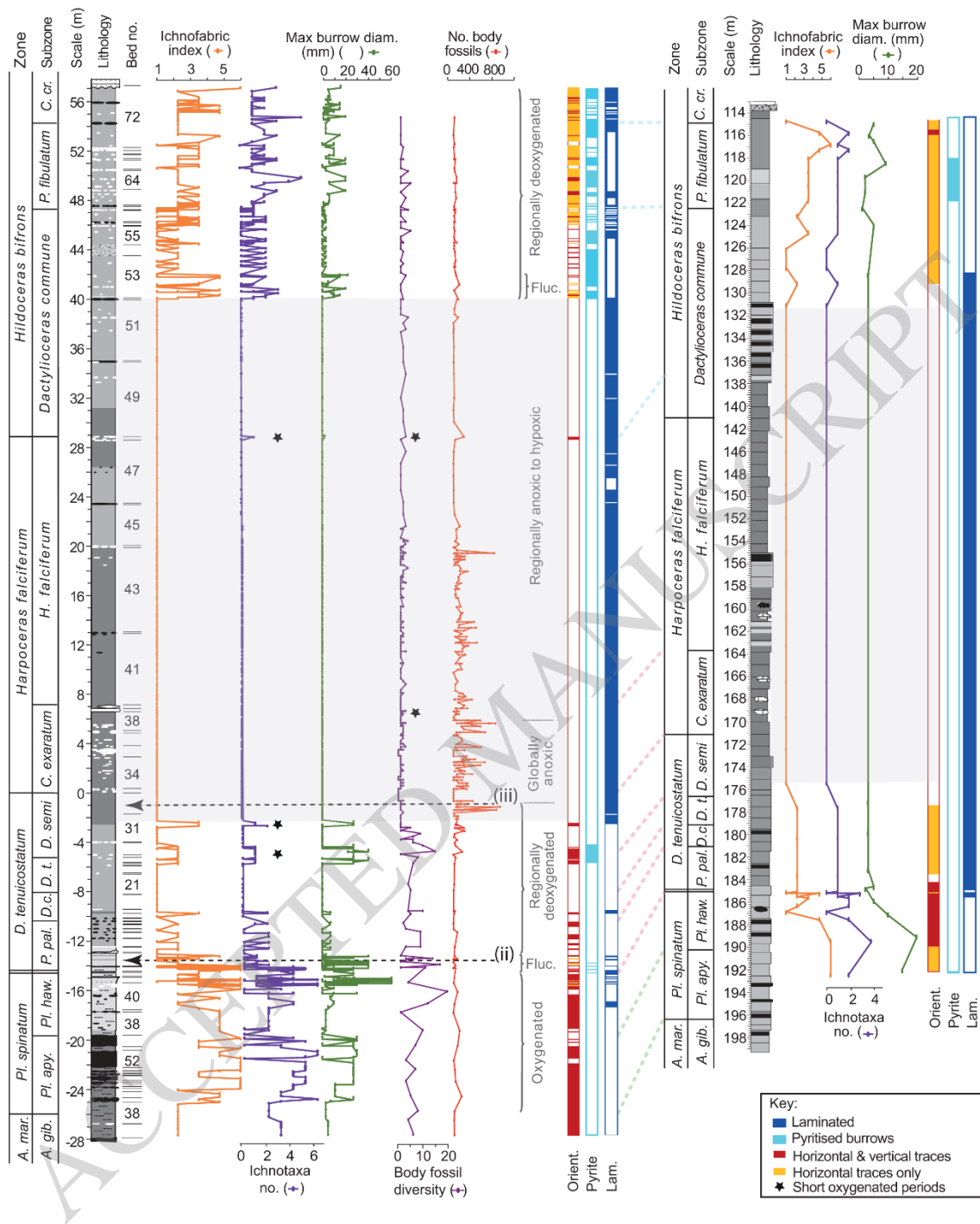


Figure 5

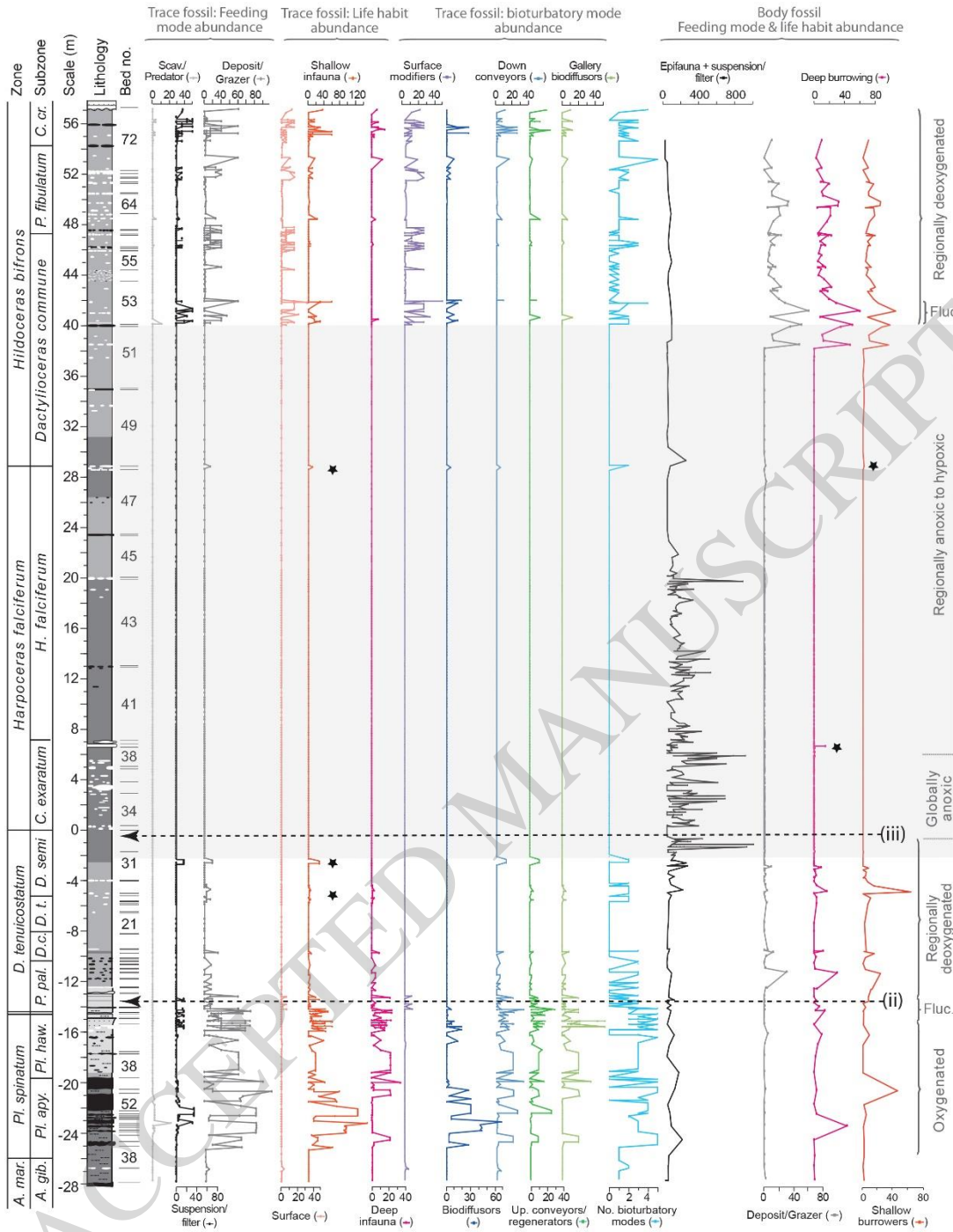


Figure 6

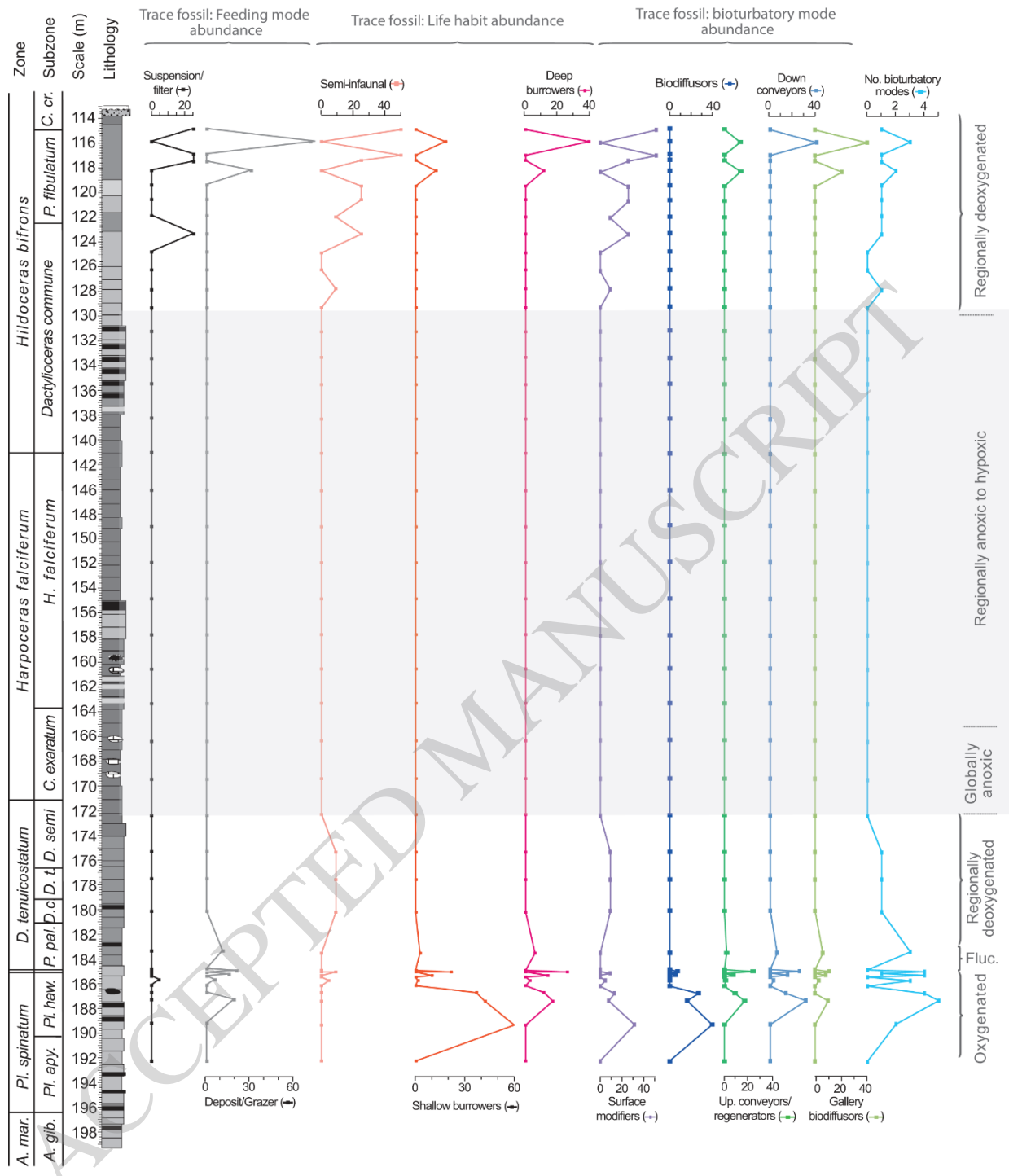


Figure 7